Review Article

Renlong Zhou, Muhammad Habib*, Muhammad Faisal Iqbal*, Naveed Hussain, Sajid Farooq, Yasir A. Haleem, Faizan Ali, and Kaleem Ullah

Twisto-photonics in two-dimensional materials: A comprehensive review

https://doi.org/10.1515/ntrev-2024-0086 received January 10, 2024; accepted July 26, 2024

Abstract: Twisted two-dimensional materials (t2DMs) such as graphene and black phosphorus are transforming the field of photonics, serving as a promising platform for the development of advanced devices that manipulate light. These materials possess multiple photonic properties that are determined by their twist angles. This article explores the profound impact of twist angles on various photonic phenomena, including nonlinear optical responses, optical absorption, plasmonics, and the influence of chirality in t2DMs. We delve into cutting-edge developments explained through Raman spectroscopy and the intriguing world of moiré excitons, as revealed through photoluminescence studies. As we explore device applications, we highlight groundbreaking advancements in photodetection, with a brief look into emerging technologies such as single-photon detectors, ultrafast modulators, light-emitting diodes, and interlayer exciton lasers. Our study extends to depict the promising future of t2DMs, emphasizing their prospective integration with other photonic systems and the discovery of novel optical phenomena in the domain of photonics. This review serves as a comprehensive guide to the dynamic field of photonics in t2DMs, highlighting current achievements and future prospects.

Keywords: twisted 2D materials, photonics, tunable, twist angle, optical response

1 Introduction

Since 2004 when graphene was first successfully isolated from graphite [1], two-dimensional (2D) materials have received a lot of interest because of their potential uses in many different sectors, including optics, electronics, and catalysis [2–5]. 2D materials have several distinctive physical features, such as the Dirac cone band structure of monolayer graphene [6-8], valley-selective polarized light absorption of transition metal dichalcogenides (TMDs) [9-11], and excellent insulation of hexagonal boron nitride (hBN) [12-15]. Benefiting from the availability of 2D monolayers, heterostructures formed by the stacking of distinct layers constitute a large new family [16]. The characteristics of a 2D heterostructure are not only a physical superposition of those of its constituent layers; rather, they are the complex result of interlayer coupling, lattice reconstruction, and twist angle, which may express and spawn unanticipated new phenomena [17]. Contrary to normal bulk materials, fabricated 2D structures exhibit several versatile features, and, in particular, the absence of surface dangling bonds substantially simplifies the construction of 2D heterostructures without additional consideration of the lattice mismatch [18,19]. In the formation of bilayers, overlapping lattice vectors from two distinct layers can generate a superlattice, creating an additional moiré periodic potential that influences electron behavior [20]. The emergence of new properties in vertically stacked monolayer materials hinges on the presence of robust interlayer coupling, which facilitates electron hopping and charge redistribution [21]. Conversely, when this coupling is

e-mail: drfaisaligbal@njust.edu.cn

Renlong Zhou: School of Physics and Information Engineering, Guangdong University of Education, No. 351 Xinggang Road, Guangzhou, 510303. China

Naveed Hussain: Department of Electrical Engineering and Computer Science, University of California, Irvine, 92697, CA, United States of America

Sajid Farooq: College of Mathematical Medicine, Zhejiang Normal University, Jinhua, 321004, China

Yasir A. Haleem: Institute of Physics, Khwaja Fareed University of Engineering and Information Technology (KFUEIT), Rahim Yar Khan, 64200, Pakistan

Faizan Ali: Institut de Ciència de Materials de Barcelona (ICMAB-CSIC), Campus UAB, Bellaterra, 08193, Barcelona, Spain

Kaleem Ullah: Department of Electrical and Computer Engineering, University of Delaware, Newark, DE, 19711, United States of America

^{*} Corresponding author: Muhammad Habib, Department of Physics, COMSATS University Islamabad, Lahore Campus, Lahore, 45550, Pakistan, e-mail: muhammad.habib@cuilahore.edu.pk

^{*} Corresponding author: Muhammad Faisal Iqbal, MIIT Key Laboratory of Advanced Metallic and Intermetallic Materials Technology, School of Materials Science and Engineering, Nanjing University of Science and Technology, Nanjing, 210094, China,

2 — Renlong Zhou et al. DE GRUYTER

weakened or disrupted, each layer retains more of its monolayer characteristics, operating more independently [22]. However, strong interlayer coupling diminishes this independence, leading to the formation of a superlattice that introduces novel long-range periodicities, altered band structures, and unique material properties [23].

In the 1950s, it was hypothesized that by combining two distinct semiconductors, several sorts of electrical devices might be created. This led to the conception of heterostructures [24]. Steele provided a theoretical description of van der Waals heterostructures (vdWHs) based on 2D materials in 1963 [25]. Due to the lack of available manufacturing techniques, the feasibility of physically absorbing a single-layer sample on the surface of the heterostructure was only explored theoretically. The photoelectric performance of graphene was improved by more than a factor of 10 when the optoelectronic characteristics of the graphenehBN heterostructure were investigated by Dean *et al.* in 2010 [26]. Since then, researchers have developed better and better 2D material transfer procedures to gain a wide range

of heterostructures [27-29]. Therefore, this phenomenon motivates scientists to dedicate themselves wholeheartedly to the topic in order to uncover versatile principles controlling the basic processes in nature [20,30-34] (Figure 1). Twisted 2D materials have a significant impact on the applications of cutting-edge electronics and optoelectronics because not only do they possess their features, but researchers may also control their properties by adjusting the twist angle [34,35]. Weak interlayer coupling at the interface was observed in twodimensional materials (t2DMs), which not only induces novel properties like bandgap opening in graphene, semiconductor band alignment, charge transfer, and new optical absorption. but also protects the fundamental characteristics of the corresponding 2D materials [36]. Cao et al. have conducted eye-catching research in the t2DMs by demonstrating magicangle twisted bilayer graphene (tBLG) [37]. By stacking two nanosheets of graphene with a relative twist of 1.1°, the authors achieved unusual superconductivity in magicangle graphene superlattices. Controversy arose when the magic-angle concept was applied to graphene-like hBN

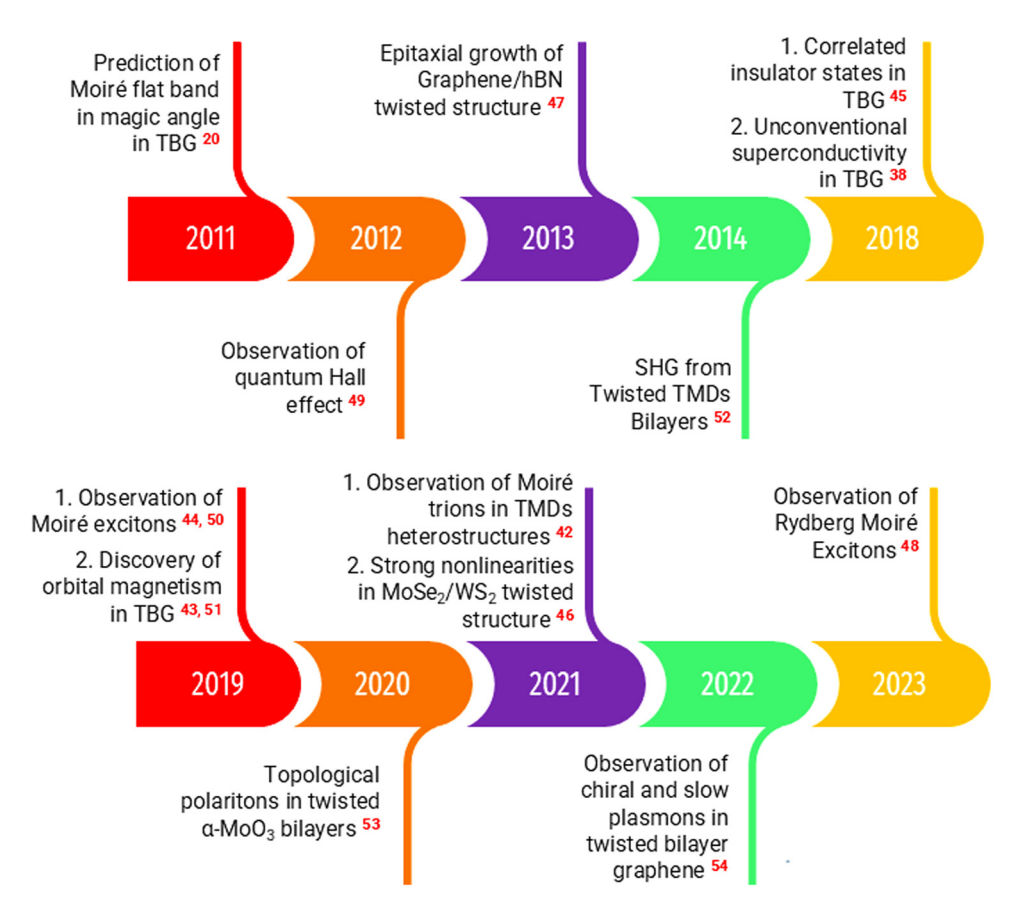


Figure 1: The timeline showcasing key advances in the study of photonics and optoelectronics within 2D materials has seen significant expansion recently, marked by numerous breakthroughs. These include the tuning of OHG, exploration of orbital magnetism, the discovery of unconventional superconductivity, advancements in the quantum Hall effect, the emergence of moiré excitons, strong mid-infrared (IR) photoresponses, light-induced ferromagnetism, and highly tunable plasmon polaritons [20,37,38–50].

systems, where the twisted angle was used to modulate intraand interlayer interactions [51-53]. These outstanding accomplishments have given rise to the twistronics field, which extends the twist concept to diverse 2D materials [32].

The purpose of this article is to highlight the immense potential of t2DMs in the field of photonics. The t2DMs, formed by stacking 2D layers with controlled twist angles, exhibit unique optical properties and offer exciting opportunities for developing advanced photonic devices. In this article, we will explore the fabrication techniques for creating twisted bilayers under various conditions, enabling precise control over the twist angle. Furthermore, we will delve into the comprehensive characterization of t2DMs' optical properties, including Raman spectroscopy, photoluminescence (PL), optical absorption, nonlinear spectroscopy, and other relevant techniques. Understanding these optical properties is crucial for harnessing the full potential of t2DMs in photonics and tailoring their behavior for specific applications. Moreover, we will examine the current state-of-the-art photonic and optoelectronic applications of t2DMs. This includes their use in photodetectors, light-emitting diodes, photovoltaics, optical modulators, and other devices. We will discuss the advancements and challenges in these applications and highlight the remarkable performance improvements and functionalities offered by t2DMs-based devices. Finally, we will discuss the future prospects of t2DMs in photonics and provide a framework for future research directions. We will explore potential areas of exploration, such as the integration of t2DMs with other materials and systems, the development of scalable fabrication techniques, and the realization of novel optical phenomena. By addressing these topics, we aim to inspire further research and innovation in the field of t2DMbased photonics, leading to transformative advancements and breakthrough technologies. This article provides a comprehensive overview of the fabrication techniques, optical properties, and applications of t2DMs in photonics. By examining the current state of the field and discussing future perspectives, we aim to shed light on the immense potential of t2DMs and inspire researchers to explore new frontiers in this exciting and rapidly evolving field.

2 Fabrication methods for t2DMs

The initial and crucial phase in researching materials science is the fabrication process. In making 2D twisted bilayer materials, two main challenges stand out: controlling the twist angle between layers accurately and establishing a clean interface. Generally, there are two preferred methods to create t2DM bilayers: the stacking approach and

the one-step chemical vapour deposition (CVD) method. In the following sections, we will explore the methods for creating t2DMs in greater detail while also drawing insights from the summary presented in Table 1, which outlines the primary approaches for t2DMs fabrication.

2.1 Two-step method stacking

One of the easiest and most reliable ways to create 2D structures is through mechanical transfer. This involves physically stacking 2D elements on top of each other. This method has been behind almost all of the major breakthroughs in twistronics, showcasing its efficiency. However, it has a significant drawback: it does not work well for large-scale production. The output is quite limited, and each sample produced generally only allows for one angle of rotation, making it tough to study how changing the angle impacts the properties of t2DMs. Fortunately,

Table 1: Key approaches to t2DMs fabrication

Method	Material	Twist angle (s) (°)	Ref.	
Stacking	Graphene	10 and 16	[54]	
·	Graphene	0.43-0.97	[55]	
	BN-graphene-BN	0-~70	[56]	
	Graphene	1.05 and 1.16	[37]	
	Graphene	0-30	[57]	
	Graphene	1.8	[58]	
	MoS ₂ /WSe ₂ , MoSe ₂ /MoS ₂	0-60	[59]	
	MoS_2	0-90	[60]	
	MoS_{2}/MoS_{2}	0-30	[61]	
	W-doped MoSe ₂	40.8-60	[62]	
	WSe ₂ /WS ₂ heterostructure	26.8-52.4	[63]	
	hBN-MoSe ₂ -hBN	~60	[64]	
	hBN/Gr/WSe ₂ /MoSe ₂ /Gr	0, 2, 30, 45,	[65]	
	heterostructures	and 60		
	MoTe ₂	0-60	[66]	
	MoSe ₂ /WSe ₂	3	[67]	
	MoTe ₂	0-60	[68]	
	MoS ₂ /WS ₂ heterostructure	0-60	[69]	
Single-	Graphene	1–30	[70]	
step CVD				
	Graphene	_	[71]	
	Graphene	30	[72]	
	Graphene	0, 30	[73]	
	Graphene	Bernal, 30	[74]	
	MoS ₂	0, 15, and 60	[75]	
	WSe ₂ /WSe ₂	1.5-60	[76]	
	MoSe ₂	7, 21, and 25	[77]	
	WS ₂	0-83	[78]	
	WS ₂	0–120	[79]	

recent innovations have started to address these issues. For instance, robots powered by machine learning can now peel off and assess samples before putting them together into the 2D shapes designed by users [80,81]. Moreover, new technology using micro-stampers has enabled what can be described as "2D printing" of these stacked structures, opening doors for potential use in large-scale industrial prototypes. Yet, despite these advancements, we still have a way to go in refining this method to be both scalable and affordable for broader use beyond specialized research environments.

In general, there are two kinds of stacking processes, exemplified by wet and dry transfer methodologies. In the wet transfer method, CVD-grown single-layer material is normally transferred onto a SiO₂/Si substrate through a simple wet-chemical process. A schematic illustration for the fabrication of twisted bilayer graphene using a wet transfer approach is shown in Figure 2(a) [54]. The first

single-layer graphene (SLG) is grown onto a Cu foil substrate followed by poly methyl methacrylate (PMMA) coating, which not only acts as a protective layer but also increases the visibility of the sample. Later, a copper substrate is etched away, and PMMA/graphene film is transferred onto a final substrate. Acetone and isopropyl alcohol treatment is performed to remove the PMMA layer. The second SLG is successively shifted onto the SLG/SiO₂/Si substrate in the same manner. In the whole process, the removal of PMMA is a key step since the interlayer interaction between graphene layers might be altered if PMMA residues are present at the top and bottom of the SLG. Due to variable morphologies of CVD synthesized SLG, it is challenging to regulate the twisting angle between graphene layers using this approach.

Besides the wet transfer approach, a partially dry transfer method was employed to create twisted MoS_2 (t- MoS_2) nanostructures, which began with similar preliminary steps [60]. The initial step consists of a formerly

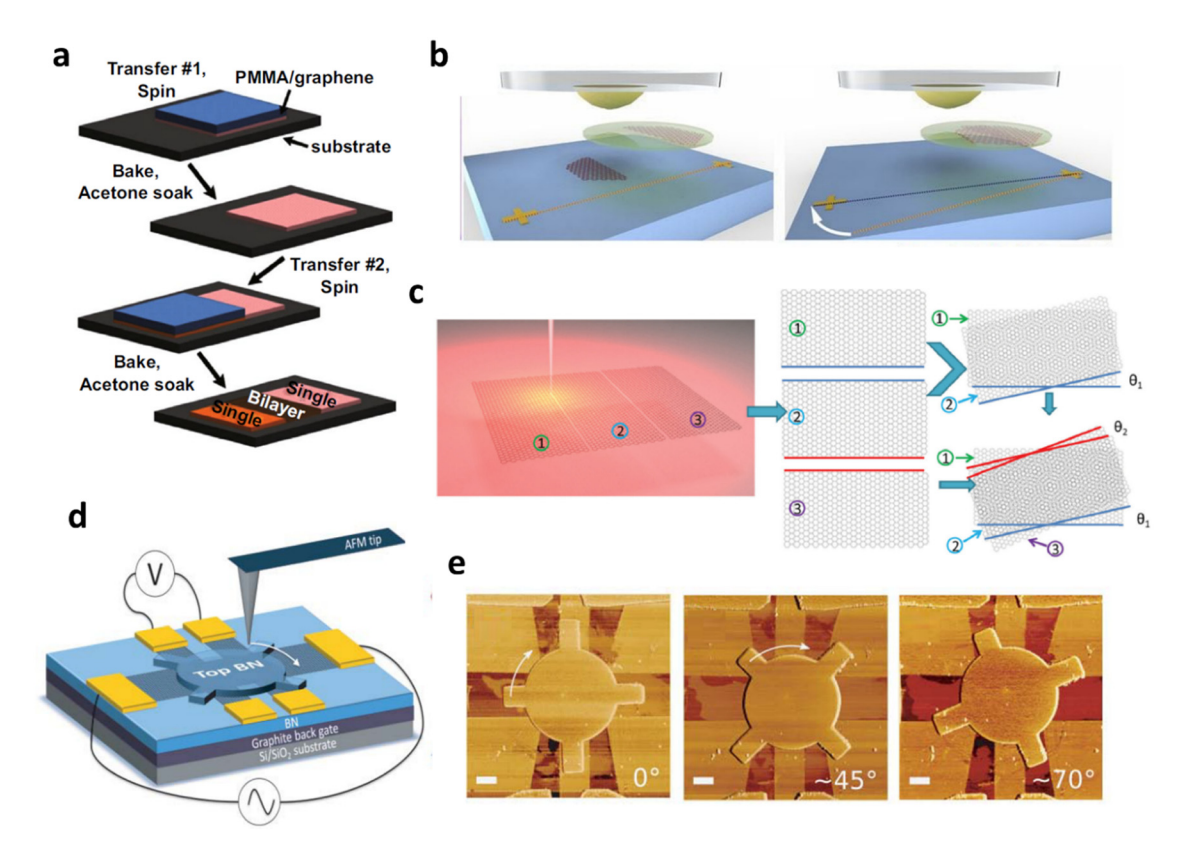


Figure 2: Representation of the two-step methods utilized in t2DMs fabrication. (a) Schematic of the process flow used in forming bilayer graphene from single-layer CVD graphene films. (b) The first section in the left image is detached from the substrate using a hemispherical handle. The second section (right image) is detached from the substrate using the same hemispherical handle. The substrate is rotated by a small angle between the two steps. Because the two flakes stem from the same graphene domain, a small twist angle is introduced between the crystal axes of the individual layers. (c) Schematic of the cutting-rotation-stacking (CRS) technique used to fabricate tBLG and double twisted trilayer graphene. (d) Schematic representation of the device and the experimental technique. (e) AFM image of a fabricated device showing three different orientations of the top BN. The angle identified in each panel is the absolute angle referenced in the AFM coordinate system (θ_A). The figure is reproduced with the permission of (a) Ref. [54], © 2013 American Chemical Society, (b) Ref. [55], © 2017 PNAS, (c) Ref. [82], © 2016 Wiley-VCH, (d, e) Ref. [56], © 2018 AAAS.

described wet chemical processing in which a MoS₂ monolayer is grown onto a temporary substrate, followed by the formation of a free-floating PMMA/MoS2 thin film. Further fabrication involves dry procedural steps. The prepared PMMA/MoS₂ layer was applied to PDMS, which is used for composite preparations as well as for stamping, and was adhered to a glass slide [83]. The baking was performed at 130°C to harden the PMMA layer. After that, the MoS₂ layer side kept downward facing and the bottom layer facing up were adjusted under the microscope. Afterwards, the glass slide was carefully brought down until it touched the bottom layer, and then PDMS was gently raised up, thus leaving behind a twisted-MoS2 bilayer structure. In the end, the t-MoS2 bilayer was annealed for 3 h at 400°C in the inert environment to consolidate the assembly. In the dry transfer method, PMMA was not incorporated between the top and bottom layers, which makes the interlayer connection very robust due to the absence of any traces of PMMA. In comparison to the wet transfer approach, the perfect removal of PMMA remnant was only accomplished in the dry transfer method because of the missing acetone treatment steps. The use of a microscope and a glass slide in this dry transfer approach makes the stacking process more precisely controlled. However, it lacks as far as sample coverage on substrate is concerned which reduces the range of twist angle of the structures created with this technique.

Figure 2(b) shows another method [55] for synthesizing bilayer graphene with a tiny twist angle by using hBN and consecutive graphene flake pickup process. The described method gives twisted heterostructures with better control over twisted angles. The elaborated process started with the growth of graphene on a substrate and then detaching of that graphene sample using a specially designed substrate called "hemispherical handle substrate" onto another substrate with metal marks for alignment and twist angle creation. The detaching process with the handle substrate is depicted in the left-side image of Figure 2(b), while its right-side image shows the detaching and transfer of the second graphene layer with a twisted angle, thus creating a tBLG structure. Due to the controlled flake pickup process and selective detachment from the exfoliation substrate, the rotationally aligned transfer technique gives greater control over crystal axis alignment as well as tiny twisting angles. The detailed process of making a hemispherical handle and the detaching process can be found in another report by the same author [84]. In a typical fabrication process, a single graphene flake, which has two distinct areas is picked up one by one with a hBN flake linked to the hemispherical handle. The hemispherical substrate was prepared with a polydimethylsiloxane (PDMS) drop and deposited onto a

glass substrate or PDMS mold. The adhesion of a fabricated hemisphere is then further improved by coating thin polymers on it. Between the first and second graphene flake pickup process, the substrate was rotated between 0.6° and 1.2° with an accuracy of 0.1°. Due to the perfect control of the twisting angle, this fabrication approach perfectly meets the demands of scientific research and applications.

Chen et al. [82] created a tBLG structure by proposing a CRS technique that is "cutting, rotating, and stacking" of graphene layers using a femtosecond laser micromachining. The schematic representation of the process is given in Figure 2(c). The SLG was mechanically exfoliated onto a SiO₂/Si substrate using a femtosecond laser and sliced into two pieces using a pair of parallel and straight cutting lines. With the manipulation of two cutting lines, the two graphene pieces were rotated by an angle and accurately layered onto a SiO₂/Si substrate using an appropriate transfer technique. As graphene films are sliced with a laser so any shape or pattern of the film can be obtained using this technique. This process provides more control over the twisting angle of tBLG than the previously mentioned procedures.

In another approach, a device consisting of a twisted BN-graphene-BN sandwiched structure was fabricated by adopting the dry transfer technique [56]. The model of the constructed device is shown in Figure 2(d), whereas Figure 2(e) is the set of AFM images of the device with different orientations of the boron nitride top layer. The fabricated device consisted of a rotatable (top boron nitride) structure, which can be rotated to exhibit tunable device characteristics. The device fabrication process was started with a dry transfer of a graphene sheet on a boron nitride layer at SiO₂/Si substrate. Successive steps of lithography and etching were performed on deposited graphene to give it a Hall bar shape. Atop graphene layer, a peculiar shape boron nitride layer was transferred to make a twistable trilayer heterostructure whose top boron nitride layer can be rotated using an AFM tip. A final round of lithography was performed to deposit the electrodes into the device.

Wang et al. [85] fabricated tBLG films by implementing the controlled folding of a SLG. This approach consists of three sub-steps: (1) the transformation of the SiO₂/Si substrate into hydrophilic and hydrophobic parts with a defined boundary, (2) the controlled delamination of SLG/ PMMA from the hydrophilic section in the water, and (3) finally the removal of the PMMA layer. By adjusting the hydrophilic and hydrophobic border folding angles, the desired twisting angle was attained. Cao et al. [37] recently reported fabrication of tBLG by vertically stacking the graphene in order to examine its superconductivity at 1.05° and 1.16° magic angles. In this procedure, one piece of SLG is

fixed, while the others are piled vertically at varying angles using the mechanical transfer method. His vertical stacking approach allowed him to achieve the necessary twisting angle in tBLG in a simple and straightforward manner. In one of the other methods [86], researchers manipulated the twist angle of the MoS₂/graphene 2D structure by pushing and twisting a monolayer MoS2 crystal with an AFM tip on graphene. When paired with high-precision rotation alignment, users were able to precisely determine the initial twist angle, hence eliminating the difficulties associated with edge recognition. In recent years, in addition to the regularly utilized etching-assisted wet or dry transfer technique, another dry peel-off transfer method has been developed. Ma et al., for instance, reported a technique for picking up and transferring 2D items using a clean stamp method aided by capillary force [87]. A thin layer of vapor (such as water vapor) is the key to enhancing the adhesion energy between 2D materials and PDMS, hence easing the pickup process. As soon as the vapor evaporates, the adhesion energy is reduced, and 2D materials may be readily released onto the desired substrate. This technique offers considerable potential for the transfer of materials on-chip. In 2018, Tao et al. [88] introduced a new peel-off technique in which water-soluble polyvinyl alcohol thin film was utilized to collect samples and consequently removed by a floating dissolution procedure. These unique transfer techniques open up new possibilities for the fabrication of large-area, high-quality t2DMs.

2.2 Single-step CVD method

The CVD method is widely utilized because it can reliably synthesize high-quality nanomaterials. Over the years, the CVD method has evolved to the point where it can now be applied to fabricate a wide variety of 2D materials and associated heterostructures [89,90]. This technique provides an opportunity to generate twisted TMD (t-TMD) bilayers without any sample transfer requirements. The one-step CVD approach is faster than the stacking method since sample transfer and stamping operations no longer remain essential. The CVD techniques for producing monolayer, bilayer, and even multilayer materials are comparable. The controlled parameters are indicative of the final result. Therefore, t2DMs bilayers must be synthesized using remarkably accurate synthesis conditions since randomly twisted bilayers are thermodynamically unfavorable and interlayer bonding takes more activation energy to form, which in turn requires a high reaction temperature. Moreover, the reaction time is crucial for promoting the synthesis of bilayer TMDs [91]. In the case of CVD-grown t-MoS₂ bilayers, for example, the ratio of MoS_2 bilayer to monolayer increased with reaction time. The twist angle has a significant impact on 2D materials characteristics, so there has been a lot of effort put in by the researchers to find a way to precisely manage it. Controlling the twist angle of CVD-grown bilayer 2D materials remains difficult owing to the complexity of the CVD environment [36]. Nonetheless, thanks to extensive research, a wealth of important data has been uncovered, opening the gateways to future controllable synthesis.

In a recent report, a twisted-WSe₂/WSe₂ structure was fabricated on a Si substrate using single-step CVD and artificial stacking techniques [76]. In particular, the authors adopted the heteroatom-assisted methodology in the CVD technique to overwhelm the stacking free energy [92]. The controlled reduction of the stacking free energy was made possible by introducing Sn atoms in the whole process, which in turn helped to prepare various WSe2 homostructures. The prepared twisted-WSe2 structures have twist angles ranging from 1.5° to 30°. During the growth, a variable temperature zone of 810-850°C was established, and hydrogen flow was also varied to achieve the required stacking. For a tungsten source, a boat containing WO₃ powder was positioned in the middle of the furnace tube along with SnO₂, while Se powder was loaded in the lowtemperature zone of the furnace. In order to get different nucleation orientations, H2 gas flow was also varied during the growth process. In the same experiment as an alternate methodology, instead of employing tungsten powder precursor, a solution of ammonium tungstate and KOH was prepared and spun coated onto a substrate. It was observed that the hydroxide present in the solution facilitates in preferred growth direction and upholds the second layer growth.

The formation of twisted-MoS2 bilayer structure on mica, fused silica, and SiO₂/Si substrates by using ambient pressure chemical vapor deposition was experimented by Liu et al. [75]. The models of MoS₂ bilayers with various twisted configurations and optical microscope images of the monolayer and twisted bilayers are shown in Figure 3(a) and (c), respectively. To transport the sulfur particles to the center of the furnace, where they could react with MoO₃, high-purity nitrogen gas was used which acts as a carrier gas. In order to boost the vertical layer-by-layer growth and decrease the nucleation rate in the early growth stage, it is necessary to optimize the CVD parameter. It was shown that the growth ratio of MoS₂ bilayers to monolayers intensifies as the growth time increases. Maximum of up to 30% yield of bilayers was achieved after 10 min of development at 700°C reaction temperature. Similarly, by employing hydrogen gas instead of argon, the t-MoSe₂ bilayer on the SiOx substrate was accomplished by using a custom-designed furnace [77]. The use of hydrogen gas was reported to speed up the chemical process

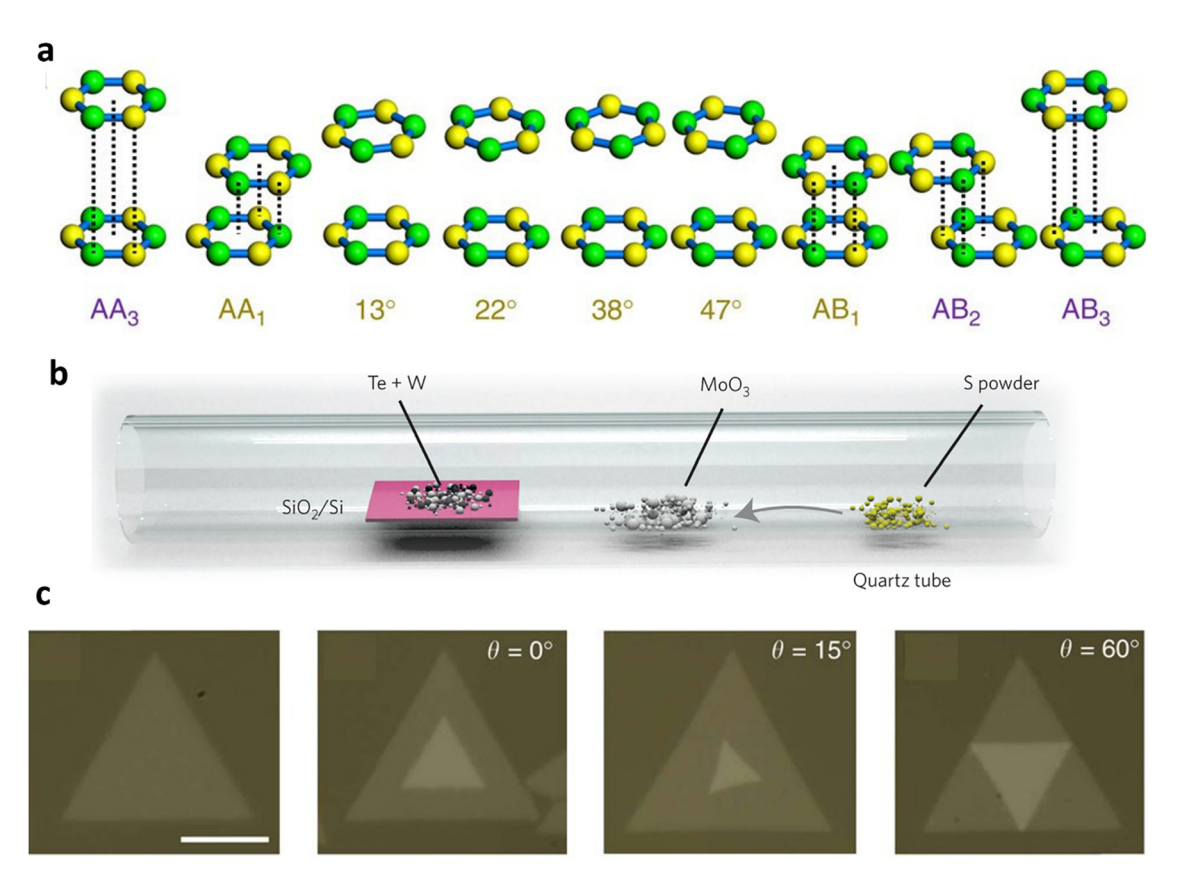


Figure 3: Representative works of one-step CVD method. (a) Schematics of MoS_2 bilayers with AA, AB, and different twisted configurations. Mo atoms are shown as green spheres; two S atoms of the same horizontal position are presented by one yellow sphere. (b) Schematic illustration of the synthesis process of MoS_2/WS_2 heterostructures. (c) Optical microscope images of monolayer and twisted bilayers MoS_2 with different twisted angles. The figure is reproduced with the permission of (a) and (c) Ref. [75], © 2014 Nature Publishing Group, (b) Ref. [97], © 2014 Nature Publishing Group.

and also serve as a reducing agent by reducing the precursors [93]. This method was equally effective for producing both monolayer and bilayer t-MoSe₂, while in another work, the t-WS₂ bilayer was found to grow at 1,100°C and at a relatively lower temperature of 850°C standard AA and AB bilayers seemed feasible [78]. It was hypothesized that at a high temperature, the top layer tries to develop with its original nucleus orientation and compensate for the angular mismatch with the bottom layer.

In the fabrication of t2DMs, various techniques significantly impact the resultant device qualities. Wet transfer methods, while cost-effective and widely used, can introduce impurities and result in less controlled twist angles, affecting device uniformity and performance [94,95]. The one-step CVD method greatly simplifies the procedure by forming twisted bilayers in a single growth step, eliminating the need for separate growth, transfer, and assembly of monolayers [34]. This method provides clean layer surfaces without polymer impurities, resulting in better device performance compared to the stack method. However, it offers less control over twist angles as the bilayer structure forms

during growth. In contrast, dry transfer methods, including PDMS stamping, offer cleaner interfaces and more precise control over material alignment, which is critical for optimizing the electronic and optical properties of devices [96]. Advanced techniques such as AFM-based manipulation provide the highest precision in twist angle and placement but are limited by their scalability and higher operational complexity [96]. Each method's suitability varies depending on the desired application and specific material properties required, making it crucial to select the appropriate technique based on the targeted device performance criteria.

3 Photonics in t2DMs

3.1 Nonlinear optical response in t2DMs

Recent studies on the nonlinear optical impact of 2D materials have shown that these materials have a greater

8 — Renlong Zhou et al. DE GRUYTER

nonlinear optical response than conventional nonlinear materials [98]. For instance, the second-order optical nonlinear coefficients of MoS₂, WS₂, and WSe₂ are two to three orders more than those of routinely used nonlinear crystals [99,100]. In a van der Waals structure, the twisted angle between the two monolayers allows further control over the optical characteristics of the 2D materials [34]. The interlayer twisting is crucial for both the tuning of the band gap and the control of the overall symmetry of the material, which has a dramatic influence on several nonlinear optical processes, such as optical harmonic generation (OHG). Therefore, the artificial staking of low-dimensional material layers

and interlayer twisting is an effective method for controlling OHG. Hsu *et al.* [48] present a comprehensive exploration of the second harmonic response in artificially stacked TMD bilayers with varying stacking angles (Figure 4(c)). The authors demonstrate that the second harmonic generation (SHG) from these twisted bilayers is a coherent superposition of the second harmonic fields from the individual monolayers, with a phase difference that depends on the stacking angle. This results in a change in the intensity and polarization of the SHG as a function of the stacking angle. The study extends to hetero-stacked WSe₂/MoS₂ and WSe₂/WS₂ bilayers, showing that the same principle applies regardless of the constituent

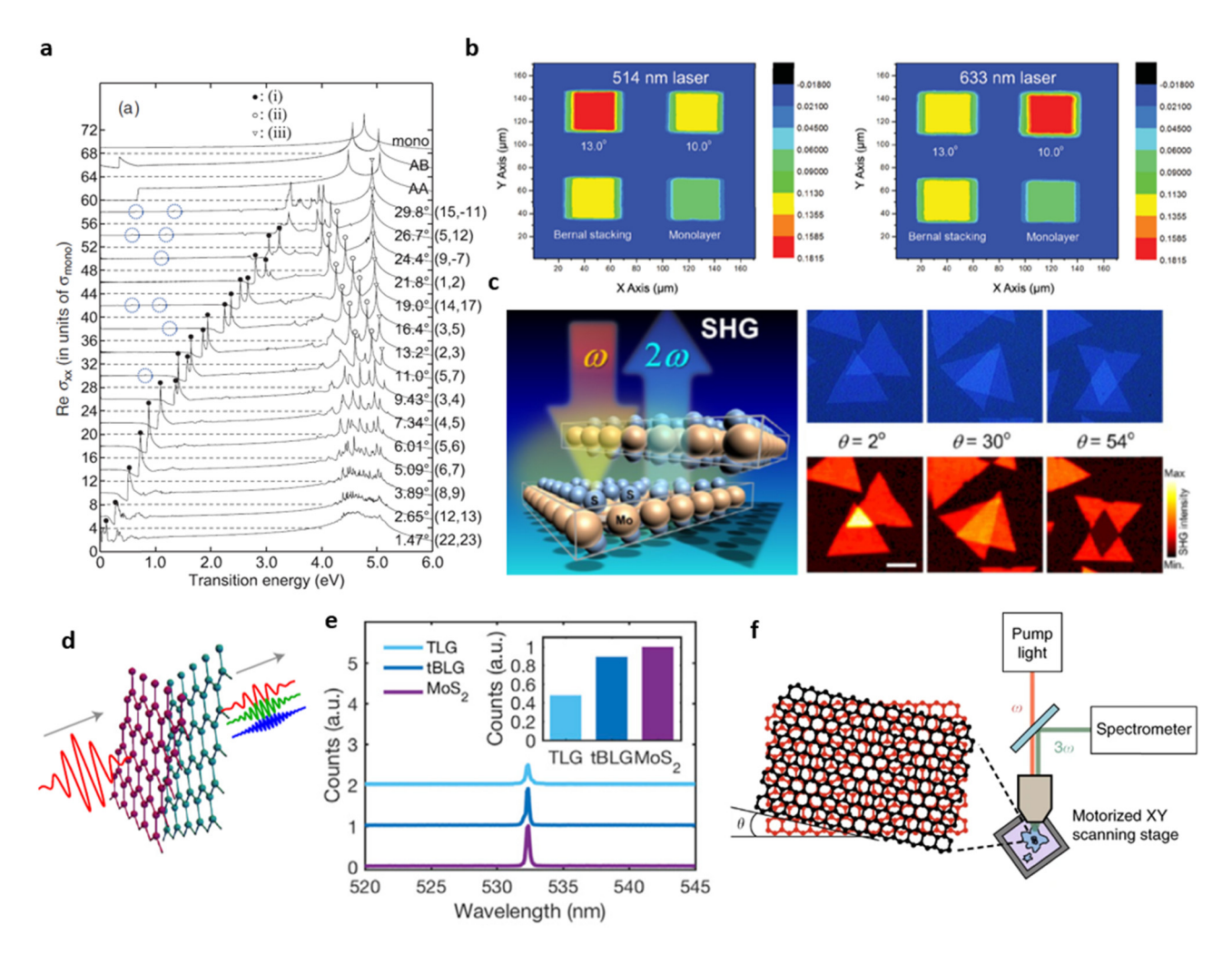


Figure 4: Nonlinear optical response and absorption in t2DM. (a) Comparison of dynamic conductivities of tBLG at various stacking angles across a broad frequency spectrum. (b) The absorption mapping visuals derived from the TIR method using laser wavelengths of 514 and 633 nm. (c) Depiction of the setup used to measure the incident laser and the mapped SHG from the twisted bilayer MoS₂ at various twisted angles. (d) A representation of how high-harmonic generation optical signals are produced from tBLG. (e) SHG spectra for trilayer graphene (light blue), tBLG (dark blue), and monolayer MoS₂ produced *via* CVD (purple). The spectra are staggered vertically for a better visual distinction. The insert provides a comparison of the SHG signal amplitude from the three materials under an identical experimental setup, excited by a 1,064 nm continuous wave (CW) laser. (f) An optical setup sketch outlining the THG measurement technique applied to tBLG. The figure is reproduced with the permission of (a) Ref. [101], © 2013 American Physical Society, (b) Ref. [82], © 2016 Wiley-VCH GmbH, (c) Ref. [49], © 2014 American Chemical Society, (d) Ref. [102], © 2020 American Physical Society, (e) Ref. [31], © 2020 Elsevier Inc., and (f) Ref. [103], © 2021 Nature Publishing Group.

layered materials. In a subsequent study [104], the authors present both experimental and theoretical evidence that interlayer twists can be used to manipulate the indirect and direct band gaps in bilayer MoS2 (2L-MoS2). This research further demonstrates that the SHG in 2L-MoS2 can be effectively controlled by adjusting the interlayer twisting angle. This finding is particularly significant as it provides a new dimension of control in the optical properties of layered materials, potentially leading to advancements in the design and functionality of optoelectronic devices. In addition to the twist angle, it is important to consider the material-dependent phase when examining SHG in t-TMD bilayers. Studies have shown that the phase delay between the fundamental and second harmonic waves varies depending on the specific materials involved. For instance, in MoS₂/WS₂ heterostructures, the phase difference significantly impacts the interference of the SHG signals, as evidenced by polarization-resolved SHG measurements [105,106]. This material-dependent phase must be taken into account to accurately understand and predict the nonlinear optical behavior of these twisted bilayer systems.

In a groundbreaking study conducted by Yang et al. [31] in 2020, it was demonstrated that by manipulating the twist angle between two layers of graphene, the secondorder susceptibility ($\chi^{(2)}$) could be altered from 0 to 28 × 10⁴ pm^2/V (4.24 × 10⁻¹⁰ m/V). This marked the first experimental demonstration of controlling SHG with twisting angles in bilayer graphene. Notably, the magnitude of $\chi^{(2)}$ in nonresonant tBLG was found to be equivalent to that of the resonant SHG of monolayer MoS2 (Figure 4(e)). Furthermore, this $\chi^{(2)}$ value remained constant across a broad range of twist angles, highlighting the robustness of this approach. This research underscores the potential of twist angle as a powerful tool for controlling nonlinear optical responses in layered materials. In a pioneering study, Ha et al. [103] presented the first significant experimental findings concerning the optical third harmonic generation (THG) in tBLG. The researchers discovered that the twist angle in tBLG significantly influences the THG. When graphene was twisted at a specific angle, an amplified THG signal was observed. This amplification occurred when the energy band gap of the van Hove singularity in tBLG matched the three-photon resonance of the incoming light. Furthermore, the researchers applied electrical gating to the samples and found an interdependent relationship between the tBLG twist angle and the THG gate voltage. In the absence of an applied voltage, the graphene seed exhibited the highest THG intensity, almost 24 times that of monolayer graphene, while the tBLG showed enhancements ranging from 3.3 to 8.2 times. This study suggests that the twist angle in tBLG introduces a new method to

regulate and enhance optical nonlinearity in tBLG, indicating its potential applications in the design of 2D-stacked materials-based nonlinear optical systems. In a theoretical study [102], researchers conducted non-perturbative computations of electron dynamics in tBLG under high-intensity laser beams. The authors assert that tBLG exhibits a richer high-harmonic generation that is not found in monolayers or conventional bilayers (Figure 4(d)). These novel harmonics carry a larger quantity of non-Dirac electrons than standard harmonics, leading to an interplay between intralayer and interlayer electron hopping. This finding suggests that the unique properties of tBLG. particularly its twist angle, can lead to novel and richer harmonic generations, further expanding its potential applications in the field of nonlinear optics and optoelectronics. As we have discussed the general principles and observed effects of nonlinear optical responses in t2DMs, it becomes imperative to delve deeper into the specific mechanisms that underpin these phenomena in different material systems. In exploring the nonlinear optical properties of 2D materials, it is crucial to understand the origin of strong nonlinearity. For tBLG, the enhanced SHG can be attributed to the unique electronic interactions and symmetry breaking induced by the twist angle. This contrasts with TMDs, where strong nonlinearity also arises from direct bandgaps and strong excitonic effects, which are highly sensitive to changes in the twist angle.

3.2 Optical absorption

The stacking pattern between the layers of 2D materials is connected to the optical absorption in 2D materials. In SLG and Bernal stacked bilayer graphene, for instance, the optical absorption in the visible region is frequency independent, and the optical absorption of SLG is 2.3% [107]. The photoconductivity of tBLG is proportional to the state density, resulting in the formation of sharp peaks in the absorption spectra [108]. Additionally, the relationship between band structure and twist angle significantly impacts the optical absorption of tBLG. As the twist angle increases from 0° to 30°, experimental observations show varied behaviors in the absorption peaks: the first peak shifts toward higher energy, the second toward lower energy, and the third remains unchanged (Figure 4(a)). Specifically, the first peak appears in the visible spectrum at larger angles, while at smaller angles, it shifts toward mid-IR wavelengths. Furthermore, studies on the photoconductivity of twisted graphene in the ultraviolet and terahertz regions reveal that while the twist angle influences optical conductivity, the spatial alignment of the layers does not affect the material's response to photoconductivity [34,109]. This indicates that optical absorption by incoming beams remains consistent regardless of the layers' relative translation when the twist angle is fixed.

The poor interaction between graphene and incident beams hinders the development of optoelectronic devices based on graphene. Chen et al. [82] suggested the use of total internal reflection (TIR) to improve the interaction between incoming beams and graphene (Figure 4(b)). By using this method, the absorption of graphene and tBLG was greatly improved. Using the CRS method, the tBLG shown was prepared on a SiO₂ substrate at stacking angles of 10° and 13°. Using a femtosecond laser, a monolayer graphene and a Bernal stacking bilayer graphene were processed into the same pattern for comparison. On several graphene samples, the optical absorption scanning imaging approach was then used. tBLG with rotation angles of 10° and 13°, Bernal stacking bilayer graphene, and monolayer graphene were all merged onto the same SiO2 substrate. The results from the examination of various samples at 514 and 633 nm are illustrated in Figure 4(b). The observation that twisted graphene with stacking angles of 13° and 10° differs greatly from other forms of graphene when excited at various wavelengths implies that twisted graphene's absorption increase is boosted. To observe an increase in the absorption of tBLG under the TIR, several graphene samples were characterized using a linear scanning approach. The optical absorption of twisted graphene is increased by about 35% compared to Bernal stacking bilayer graphene. Due to the higher optical absorption of graphene under TIR, the absorption peak of graphene due to the twist angle can be detected clearly, allowing TIR absorption imaging to determine the stacking angle of bilayer graphene. The authors conducted absorption imaging tests on irregular samples with varied rotation degrees in order to validate the angular resolution of absorption imaging for irregular patterns. The results suggested that monolayer graphene, bilayer graphene with Bernal stacking, and twisted graphene with varied stacking angles may be identified by optical absorption in TIR mode. Consequently, the graphene twist angles may be identified using this method.

3.3 Plasmonic in t2DMs

Plasmonic in twisted layered structures is an exciting and rapidly developing field that focuses on the manipulation and control of plasmons in materials with layered structures. Plasmons are collective oscillations of electrons in a

material, and their interaction with light offers unique opportunities for enhancing light-matter interactions at the nanoscale. In twisted layered structures, the formation of moiré superlattices introduces spatially modulated electronic properties, giving rise to intriguing plasmonic phenomena [110]. One of the key aspects of plasmonic in twisted layered structures is the ability to engineer and control the plasmonic resonances by adjusting the twist angle between the layers. The twist angle plays a crucial role in determining the electronic band structure and the spatial distribution of charge density, which directly affects the plasmonic behavior. By tuning the twist angle, researchers can tailor the plasmonic resonances to operate at desired frequencies, enabling applications in various spectral regions, such as visible, IR, and terahertz [111]. In twisted layered structures, localized plasmon modes can arise due to the confinement of charge density within the moiré unit cell. These localized plasmons exhibit strong field confinement and can enhance light-matter interactions within the nanoscale regions.

Huang et al. [50] have made a noteworthy advancement in the realm of plasmonics in twisted layered materials by successfully observing chiral and slow plasmons in tBLG through the use of IR nano-imaging techniques. The research underscores that by manipulating the twist angle and doping level of tBLG, it is possible to adjust the properties of plasmons, thereby paving the way for the creation of plasmonic devices with customized optical responses. The discovery that chiral plasmons originate from the Berry curvature of the flat bands in tBLG offers a fresh perspective on the relationship between topology and plasmonics in 2D materials. The theoretical model proposed in the study [50], which explains the enhancement of optical chirality in tBLG based on the Berry curvature and the amplitude of the electric field of circularly polarized light, could serve as a roadmap for future research on the creation and fine-tuning of chiral plasmonic devices. tBLG is formed when two graphene layers are slightly rotated relative to each other (approximately 1°) and exhibits unique singleparticle and many-body properties due to the moiré superlattice induced by the twist. These properties are distinct from those of a single graphene layer. In this study [112], the researchers utilized mid-IR near-field optical microscopy to probe the collective excitations, or plasmons, of tBLG at a spatial resolution of 20 nm. They identified a propagating plasmon mode in charge-neutral tBLG for twist angles (θ) between 1.1° and 1.7°. This plasmon mode differs from the intraband plasmon observed in SLG and is interpreted as an interband plasmon associated with the optical transitions between minibands that originate from the moiré superlattice. The dispersion details of the plasmon are directly linked to the electron dynamics within the moiré superlattice, providing insights into the physical properties of tBLG. These properties include band nesting between the flat band and remote band, local interlayer coupling, and energy losses. The researchers observed a significant reduction in interlayer coupling in regions with AA stacking, suggesting screening due to electron–electron interactions.

In this work [113], a lithography-free photonic crystal for plasmons in tBLG was demonstrated (Figure 5(c) and (d)). The tBLG, formed by rotationally misaligned graphene layers, exhibits periodic variations in optical response due

to the modification of electronic structures at moiré domain walls (solitons). The most notable feature of the modified electron dispersion is the emergence of chiral one-dimensional states, which are topologically protected. Optical transitions involving these states produce an enhancement of local optical conductivity across the solitons. Using IR nano-imaging experiments, the researchers visualized the interference between surface plasmon polaritons propagating in solitonic networks and predicted the formation of a full plasmonic bandgap. This approach leverages local changes in the electronic band structure of the plasmonic medium, a quantum effect, to control optical

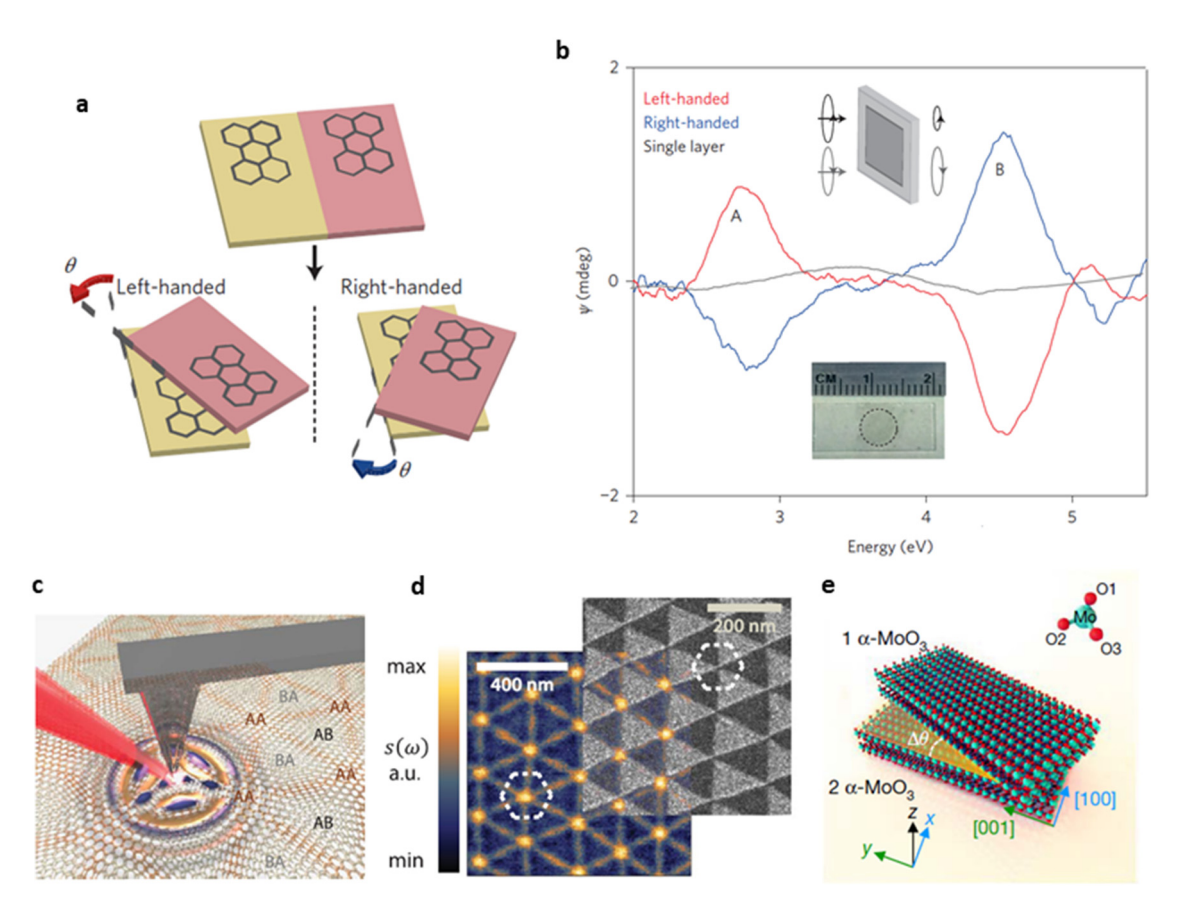


Figure 5: Interplay of chirality and plasmonic in t2DMs. (a) A schematic of the chiral stacking technique utilized to create left- and right-handed tBLG films, separated by a mirror plane (depicted as a vertical line). (b) The ellipticity (Ψ) spectra, otherwise known as the CD spectra, taken from a set of chiral tBLG films with a twist angle (θ) of 16.5° (red for left-handed, blue for right-handed), and also from SLG (represented in gray). The CD spectra for both left- and right-handed tBLG display two distinct strong peaks, labeled Peaks A and B. The lower inset displays a photograph of a tBLG film (indicated area; 5 mm in diameter) positioned on a fused silica substrate. The upper inset shows a schematic for Ψ measurements, illustrating how tBLG differentially absorbs left- and right-handed circularly polarized light. (c) The setup for the IR nano-imaging experiment. AB, BA, and AA labels signify the recurring stacking types of graphene layers. (d) (Left) The photonic crystal formed by the soliton lattice through nano-light visualization where contrast results from enhanced local optical conductivity at solitons. (Right) A dark-field transmission electron microscope (TEM) image of a tBLG sample, displaying contrast between AB and BA triangular domains. Dashed hexagons signify unit cells of the crystals and a.u. represents arbitrary units. (e) A schematic of twisted bilayer α-MoO₃. Here, the top layer (1 α-MoO₃) and bottom layer (2 α-MoO₃) have thicknesses d1 and d2, respectively. The *x* and *y* axes align with the [99] and [001] directions of 2 α-MoO₃. The twist angle $\Delta\theta$ is defined as the anticlockwise rotation of 1 α-MoO₃ relative to 2 α-MoO₃ by the indicated amount. The figure is reproduced with the permission of (a) and (b) Ref. [114], © 2016 Nature Publishing Group, (c, d) Ref. [113], © 2018 American Association for the Advancement of Science (AAAS), € Ref. [49], © 2020 Nature Publishing Group.

phenomena, offering a fundamentally quantum approach for manipulating plasmons. Hu et al. [49] extend the concept of plasmonic in twisted bilayer materials, specifically focusing on phonon polaritons in α -MoO₃ bilayers (Figure 5(e)). The authors demonstrate how the twist angle between the layers can be manipulated to control the photonic dispersion of these polaritons, similar to the control of electronic band structure in tBLG. This manipulation leads to phenomena such as topological transitions and the emergence of topological polaritons. The article also suggests the possibility of achieving similar control in a stack of hyperbolic metasurfaces formed by densely packed graphene nanoribbons. providing a potential pathway for further exploration of plasmonic in twisted layered materials. Phonon polaritons in α-MoO₃ are highly anisotropic, meaning they propagate only along certain directions in the basal plane. By twisting stacked α-MoO₃ slabs with angles ranging from 0° to 90°, the researchers were able to achieve various wavefront geometries and polariton topological transitions [115]. This tunability is attributed to the electromagnetic hybridization between directional phonon polaritons in the top and bottom α-MoO₃ slabs, which strongly depends on the twisting angle. This work suggests the potential to produce polariton nano-light with tailored propagating properties and photonic density of states for various nanophotonic functionalities. The exploration of plasmonic in twisted layered materials, such as graphene and MoO₃, has revealed promising pathways for controlling nano-light. By exploiting the quantum properties of these materials and their unique responses to twisting, researchers have demonstrated the potential to create photonic crystals and highly confined plasmon polaritons. These discoveries not only enhance our understanding of lightmatter interactions at the nanoscale but also pave the way for the development of advanced nanophotonic devices and systems.

3.4 Chirality in t2DMs

In the context of layered materials, such as graphene and other 2D structures, chirality becomes particularly crucial when these materials are twisted. Such twists introduce rotational asymmetry, leading to structures known as twisted bilayer materials. The interplay between the intrinsic properties of 2D materials and the introduced twist results in novel and intriguing chiral properties [116]. For example, the development of chiral tBLG highlights the tunability and versatility of these structures. The controllable rotation between layers and the polar orientation within the layers enable manipulation of

the optical and electronic properties, including the absorption of circularly polarized light.

Kim et al. [114] introduced a novel approach involving the precise layer-by-layer assembly of 2D materials. They meticulously controlled the rotation and polarity between the layers to construct materials with modifiable chiral properties. Using this method, they developed tBLG samples that exhibited either left- or right-handedness. This type of graphene demonstrated exceptional properties, such as one of the highest reported intrinsic ellipticity values (6.5 deg µm⁻¹), and a strong circular dichroism (CD) with the ability to tune the peak energy and sign through the adjustment of the stacking angle and polarity. They deduced that these distinctive chiral traits stemmed from a substantial in-plane magnetic moment that arose from the optical transition between layers. Moreover, the authors successfully programmed the chiral attributes of these atomically thin films layer-by-layer by crafting threelayer graphene films with structurally regulated CD spectra. The fabrication process started with growing a monolayer graphene with a uniform crystalline orientation. This layer was then sectioned and stacked layer by layer with a carefully controlled twist angle (Figure 5(a)). The rotation was either anticlockwise or clockwise, leading to the formation of left- or right-handed films, respectively, that are linked by a mirror plane. The resulting chiral tBLG films had twist angles and handedness that were uniformly managed over several millimeters, thereby achieving a high yield of interlayer coupling. The electronic, electrical, and optical characteristics of the tBLG could be modulated using the twist angle, which opened up possibilities for studying the intrinsic chiral properties of bilayer graphene. They found that this twisted graphene had a pronounced CD, absorbing left and right circularly polarized light at disparate rates (Figure 5(b)). Compared to the CD spectra of SLG, the twisted bilayer variant displayed two prominent peaks in the CD spectra, one positive and the other negative. Importantly, they noticed that the ellipticity (Ψ) switched its sign depending on the handedness of the tBLG, signifying a direct correlation between the CD spectra and the structure of the tBLG.

Chirality in twisted vdWHs, such as tBLG, presents a unique quantum property that is characterized by the rotational mismatch between layers, leading to the emergence of chirality due to the quantum nature of interlayer coupling. Stauber *et al.* [117] demonstrated that chiral plasmons, characterized by a longitudinal magnetic moment accompanying the longitudinal charge plasmon, result in electromagnetic near fields that are also chiral. Particularly in tBLG, the researchers [117] estimated that the near-field chirality of screened plasmons can be several

orders of magnitude larger than that of the related circularly polarized light, further exhibiting itself in a deflection angle that is formed between the direction of the plasmon propagation and its Poynting vector. This property breaks all mirror plane symmetries and does not rely on the disruption of time-reversal symmetry, suggesting potential applications in catalyzing chemical reactions without requiring the alteration of external conditions, such as the introduction of a magnetic field. The authors identified substantial field enhancements, particularly with acoustic plasmons, pointing toward the potential for chiral plasmoninduced chemistry. This phenomenon is applicable across twisted van der Waals structures, as interlayer moiré coupling induces a chiral response, bestowing surface plasmons with a chiral character. Unlike traditional concepts in chiral plasmonic, the near-field chirality in this context has a quantum origin tied to the interlayer coupling between atomic layers, thereby negating the need for nanofabrication of metallic chiral structures. This breakthrough paves the way for expanding this approach to other 2D materials beyond graphene and suggests a novel methodology for creating macroscopic chiral platforms for a range of applications, including optics, sensing, chemistry, and more. Potential practical implications range from enantioselective synthesis of amino acids to pioneering catalyzed reactions of chiral molecules. The researchers' findings hint that twisted vdWHs might offer a novel platform to enhance enantiomer-selective physio-chemical processes in chiral molecules without the need for a magnetic field.

3.5 Raman spectroscopy in t2DMs

Raman spectroscopy is a powerful technique widely used for the characterization of t2DM materials [118]. Twisted layered materials, such as graphene, TMDs, and other vdWHs, exhibit unique Raman spectra due to the interlayer coupling and the formation of moiré superlattices. Raman spectroscopy provides valuable insights into the structural, electronic, and vibrational properties of these materials, offering a nondestructive and highly sensitive analytical tool for studying

Table 2: Raman scattering in twisted layered structures

Studied twisted system	Excitation laser (nm)	Twist angle(s) (°)	Key observations
WSe ₂ bilayers [119]	532	0-60	Breathing mode Interlayer shear mode for mapping of moiré superlattices
Graphene bilayers [120]	488, 532, and 632	0–30	G-band and 2D band Origin of van Hove singularities
Graphene bilayers (tB ₁ , and tB ₂) [121]	514	In tB_1 23–27 when $T \le 300$ K and 3–8 for $T > 300$ K and in tB_2 , 13–16 for 80–200 K and 5–9 for 250–450 K	 Observed G, D, 2D and D + D" Phonon bands and studied temperature dependence of twist angle
WS ₂ bilayer [122]	488	0–60	Probing angle-dependent interlayer coupling using A_{1g} , and E_{2g} Raman modes
Graphene bilayers [123]	633	0.01–2.6	Studied localization of phonons by monitoring G and G' bands
MoS ₂ bilayers [124]	532	0-60	 Used interlayer shearing (22 cm⁻¹) and breading (36 cm⁻¹) modes A_{1g}, E_{2g} and 2LA(M) interlayer Raman modes to prob interface properties
Graphene bilayers [70]	514	0–30	The synthesis process of bilayers graphene was examined by the variation of G and 2D bands
MoS ₂ bilayers [125]	532	0–30	The moiré phonons and strain-coupled phonons A_{1g} , FA_{1g} and E_{2g} are observed
W-doped MoSe ₂ bilayers [62]	532	33.2-60	Variable local stacking and interlayer coupling were studied using breathing modes B ₁ at 32 cm ⁻¹ and B ₂ at 27 cm ⁻¹ and shear mode at 19.2 cm ⁻¹
Stacked WS ₂ bilayers [78]	532	0-83	Coupling and interlayer excitonic study with the help of 2LA and A_{1q} modes
Stacked black phosphorus [126]	441.6	7, 50, 75, 80, and 90	$A_g^1,\ A_g^2,\ and\ B_{2g}$ assisted in examining interlayer coupling effect for optical applications

twisted 2D systems [127] (Table 2). One of the primary advantages of Raman spectroscopy for t2DMs is its ability to probe the lattice vibrations and phonon modes. The interaction of the incident laser light with the material induces inelastic scattering, leading to the generation of Raman signals at different frequencies [122,128-130]. The Raman spectra of twisted layered materials exhibit characteristic features, including the presence of moiré modes, hybridized phonon modes, and replica bands [131]. These features arise from the modified lattice structure and the interlayer interactions, providing valuable information about the twist angle and the electronic band structure. The moiré modes observed in Raman spectra of t2DMs are particularly significant. These modes arise from the periodic modulation of the lattice and result in additional peaks in the Raman spectrum [132]. The intensity, frequency, and linewidth of these moiré modes depend on the twist angle, the interlayer coupling, and the local environment. By analyzing the moiré modes, researchers can determine the twist angle and gain insights into the interlayer interactions and strain effects in t2DMs [133].

14

Raman spectroscopy also allows for the investigation of electronic properties in twisted layered materials. The interlayer coupling and the presence of moiré superlattices introduce additional electronic states and modify the electronic band structure of the material [132]. This, in turn, affects the Raman scattering processes and leads to changes in the Raman spectra. By analyzing the Raman shifts, intensity changes, and polarization-dependent measurements, researchers can gain valuable information about the electronic properties, such as the bandgap, Fermi level, and the presence of excitonic states in t2DMs [127]. Furthermore, Raman spectroscopy provides insights into the strain distribution and the local environment in t2DMs. The lattice mismatch and the twist angle introduce strain variations across the material, which can influence the vibrational properties and the Raman signals. By mapping the strain distribution using Raman spectroscopy, researchers can characterize the strain fields, investigate strain-induced phenomena, and study the strain relaxation mechanisms in twisted layered materials [134].

In this work [119], the authors successfully demonstrate that low-frequency (LF) Raman scattering can be used to probe the local moiré period in twisted bilayer TMDs through both the interlayer breathing mode and moiré phonons. The researchers show that moiré superlattice homogeneity can be conveniently mapped across a large sample area, allowing them to identify regions of different contact, atomic reconstruction, and rotational sliding. The authors address the limitations of existing imaging techniques, like transmission electron microscopy (TEM) and scanning probe microscopy, by presenting a more convenient, non-invasive method. This method provides better compatibility with subsequent device

fabrication and transport measurements, with a twist-angle resolution of about 0.1°. Furthermore, they reveal that atomic reconstruction, previously expected only in bilayers with small twist angles, can occur even in bilayers with larger twist angles, thus expanding our understanding of these structures. Figure 6(e) demonstrates the twist-angle-dependent Raman spectra of twisted bilayer WSe₂ samples, revealing a breathing mode that is initially independent of twist angles up to 3°, but starts to shift with increasing angle from 4° onwards. Figure 6(f) summarizes the breathing-mode frequencies as a function of twist angles, showing a clear correlation with the calculated moiré period, highlighting the significant impact of twist angles on the vibrational properties of the material.

DE GRUYTER

The application of Raman spectroscopy in studying twisted bilayer TMDs has provided a deeper understanding of their properties and interlayer interactions. The study by Huang et al. [60] examined a twisted MoS₂ bilayer with various twist angles but observed no significant angledependent Raman signal. However, a later study by Liu et al. [75] on CVD-grown MoS2 found a constant redshift of the E_{2g} peaks and a twist-angle-dependent blueshift of the A_{1g} peak. The separation between these peaks was found to be an effective indicator of mechanical interlayer coupling. Similar Raman spectroscopic investigations were also carried out on twisted WS₂ bilayers [78], revealing characteristic differences related to phonon vibrations and interlayer coupling. In addition, Raman spectroscopy has also been used to investigate the interlayer coupling in bilayer heterostructures like WSe₂/WS₂, demonstrating the effect of interlayer coupling between the different materials [63]. LF Raman spectroscopy, which has a high sensitivity for probing van der Waals interlayer coupling, was utilized to study twisted MoSe₂ bilayers [62]. The LF Raman spectra showed a highly sensitive response to interlayer coupling, with minor twist angle deviations leading to substantial changes in the spectra. Likewise, LF Raman spectroscopy applied to t-MoS₂ bilayers revealed a highly responsive LF mode to the interlayer stacking and coupling [124]. Overall, these works highlight that LF Raman spectroscopy can offer more effective insights into interlayer stacking and coupling due to its detailed and comprehensive characterization capabilities.

Raman spectroscopy has been frequently employed to investigate tBLG and other graphene heterostructures [132]. It has revealed new Raman peaks associated with phonons within the Brillouin zone (BZ) of graphene, corresponding to the reciprocal unit vectors of the moiré superlattice. Other interesting effects include a dramatic increase in the intensity of the G-band for certain laser excitation energies and twist angles and resonance mechanisms activating the

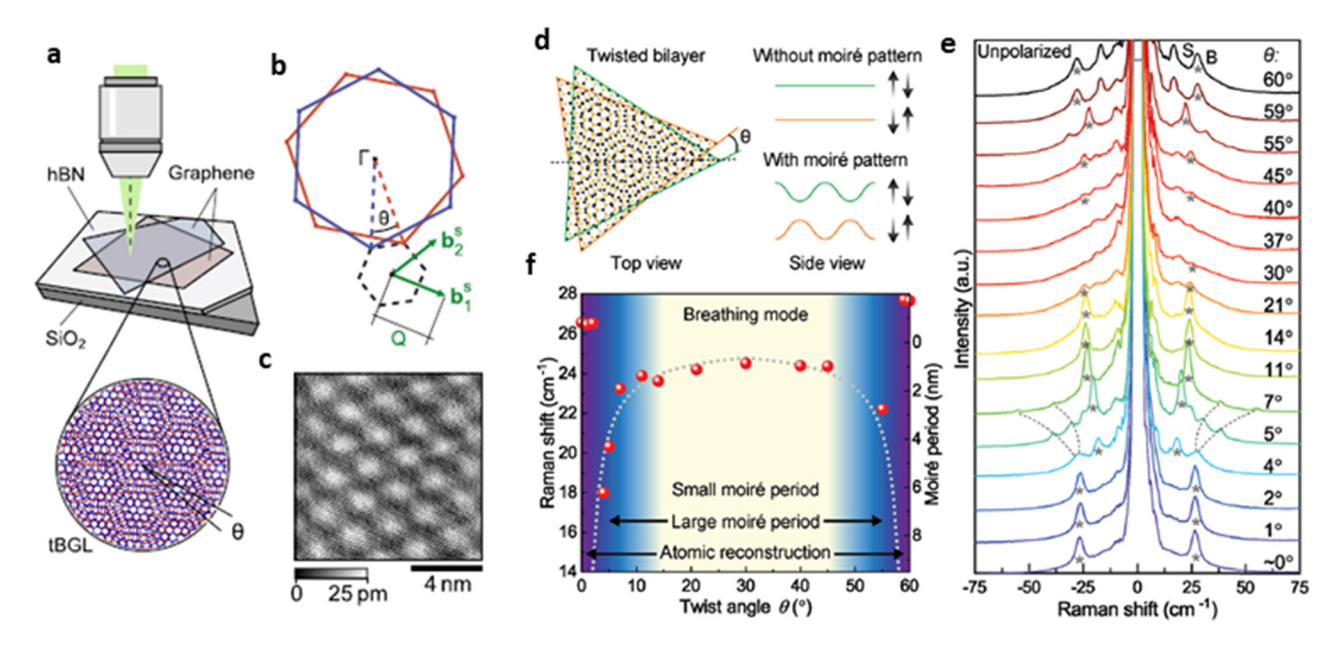


Figure 6: Implementation of Raman spectroscopy in t2DMs. (a) Graphic representation of the experimental setup for spatial Raman mapping of tBLG situated on hBN. The smaller inset highlights the developed moiré pattern for a predetermined twist angle θ . (b) The emergence of a mini-BZ, signified by reciprocal lattice vectors b1 and b2, owing to the supplementary periodicity of the superlattice. (c) A scanning tunneling microscopy image with atomic precision of the crafted tBLG structure with a twist angle of 7.5°, inferred from the moiré periodicity. (d) Depiction of twisted bilayer WSe2 in physical space and the low-energy interlayer breathing mode in the presence and absence of a moiré pattern. The green and orange lines outline the terrain of the upper and lower layers, respectively. (e) The LF Raman spectra of bilayer WSe₂ as mapped against twist angle. The interlayer breathing modes are signified by asterisks, while the dashed lines point out the moiré phonon. Breathing mode (b) and shear mode (S) from the 2H natural bilayers (60°) are provided for reference. (f) The twist angle reliance of the breathing-mode frequency (displayed as red dots) precisely demarcates three regimes of twist angles: atomic reconstruction (purple) where the breathing mode becomes more rigid; large moiré unit cells (blue) where the breathing mode eases with a growing moiré period; and small moiré unit cells (yellow shade) where the breathing mode remains almost unchanged with twist angle. The gray-dotted curve outlines the twist-angle reliance of the moiré period. The error from peak fitting is smaller than the diameter of the spheres. The figure is reproduced with the permission of (a)–(c) Ref. [142], © 2022 IOP Publishing Ltd, (d)–(f) Ref. [119], © 2021 Wiley-VCH GmbH.

appearance of extra peaks, with both intralayer and interlayer electron-phonon processes involved [135].

tBLG is created by superposing two periodic 2D structures at a mismatch rotation angle, resulting in a moiré pattern superlattice [136]. This pattern's size depends on the twist angle, and when the layers consist of different materials, the effect also depends on each layer's lattice parameters [133]. tBLG exhibits novel properties due to the coupling between the Dirac cones of the two layers, giving rise to van Hove singularities in the density of electronic states, which vary with the twist angle. The tBLG phenomenon, especially the so-called magic angle around 1.1°, has sparked much interest due to the appearance of strongly correlated phases [37]. This is caused by a flattening of the electronic bands near the Fermi energy, leading to phenomena like superconductivity when electron-electron interactions dominate. Twisting angles in tBLG provide a way to create novel tunable quantum devices, thanks to interlayer and intralayer electron-phonon interactions, which are crucial in condensed matter physics [137].

In 2010, Gupta et al. [138] reported the presence of a new, non-dispersive peak in the Raman spectra of a folded graphene monolayer. The research attributed this result to the static interlayer perturbation between layers activating a finite wavevector that conserves momentum with a phonon through double-resonant Raman (DRR) scattering. Righi et al. [139] later found several additional peaks, associating these extra features with phonon modes from inside the graphene BZ that become Raman-active due to the twisted neighboring graphene layers. Each family of peaks could be linked with specific rotational angles in moiré patterns. Carozo et al. [140] attributed new peaks near the G-band position to intervalley and intravalley DRR processes, estimating the resonance energies as a function of the twist angle for these two processes. Both processes considered in their work are examples of intralayer electron-phonon scattering as they occur within the same graphene layer.

Several innovative methodologies have been employed to understand the vibrational properties of tBLG via Raman spectroscopy. One study [141] detailed a fabrication method for tBLG using direct transfer of CVD-prepared graphene onto another epitaxial layer on copper foil, reducing interface contamination and observing the effects of thermal annealing on the tBLG through Raman spectroscopy. Another research [135] showed the use of superlattice-induced Raman scattering to probe the phonon dispersion in tBLG, and even observed layer breathing vibrations (ZO phonons). Additionally, the application of confocal Raman spectroscopy [142] was demonstrated in a third study to spatially map the twist angle in stacked bilayer graphene (Figure 6(a)-(c)). Lastly, a comprehensive study [143] was carried out to synthesize tBLG using CVD and characterize twist angles using TEM and Raman spectroscopy, while also employing large-scale molecular dynamics simulations to compare theoretical and observed vibrational frequencies. These investigations, along with numerous other studies, have greatly expanded our understanding of the twisting vibrational properties of graphene.

3.6 PL and moiré exciton in t2DMs

PL spectroscopy is a powerful characterization technique widely employed for the investigation of t2DMs (Table 3). This technique provides valuable insights into the optical

and electronic properties of these materials, offering a non-destructive and highly sensitive means to study their excitonic states, band structures, and energy dynamics [144]. In the case of t2DMs, the interlayer coupling and the formation of moiré superlattices introduce unique optical properties that can be probed using PL spectroscopy [32]. The interplay between the twist angle and the electronic band structure leads to the modification of excitonic states and the emission properties of the material [145]. One of the primary advantages of PL spectroscopy for t2DMs is its ability to study excitonic effects. The strong electron-electron interactions and the reduced dimensionality in 2D materials give rise to excitons, which are bound electron-hole pairs. The twist angle and the moiré superlattice can significantly alter the excitonic states, their binding energies, and their spatial localization. By analyzing the PL spectra, researchers can extract information about the exciton energies, their spatial distribution, and the effects of interlayer coupling on their properties [146]. Furthermore, PL spectroscopy enables the investigation of the band structure and electronic properties of t2DMs [144]. The interlayer coupling and the presence of moiré superlattices introduce new energy dispersions and modified electronic states. By studying the PL spectra, researchers can obtain insights into the bandgap, Fermi level, and the presence of localized or delocalized electronic states.

Table 3: PL spectroscopy in twisted layered structures

Studied twisted system	Excitation laser (nm)	Twist angle(s) (°)	Key results
Stacked WS ₂ bilayers [78]	532 and 457	0, 13, 30, 41, 60, and 83	 Direct transition at 1.9 eV The PL intensity of 30° twisted sample was 22 times stronger than the sample with a twist angle of 0° Indirect transitions for 0° and 60°
MoS ₂ bilayers [147]	532	0.5	 A-exciton energy 2 eV A-exciton intensity suppressed by 50% as compared to single layer B-exciton energy 1.85 eV
Spiral WS ₂ [148]	532	4.5	Observation of two peaks I and II related to the luminescence of moiré exciton
WSe ₂ /WSe ₂ and WS ₂ / MoS ₂ [149]	532	1, 28, and 59 for homobilayer 2, 26, and 58 for hetero-bilayer	 Homobilayer showed the strongest PL peak at 1.68 eV for a twist angle of 28° The intensity was suppressed for twist angles 1° and 59°, and a read shift in peak energy was observed Decoupled PL peak observed at 1.64 eV at a twist angle of 26° in hetero-bilayer A downshift to 1.58 eV was observed for twist angles 2° and 58°
MoS ₂ and MoSe ₂ flowers like bilayers [150]	532	0, 16, 21, 25, 30, 36, 45, and 60	 Strong direct PL emission in MoS₂ Indirect transition at 0° and 60° and weaker PL intensity In MoSe₂ indirect to direct transition occurred at 56°

Additionally, the linewidth and intensity of the PL peaks provide information about the scattering processes and the carrier dynamics in the material [151].

The modification of the electronic band structure of TMD bilayers through interlayer coupling has become an important area of study. In this context, Zheng et al. [78] delved into the investigation of twisted WS2 bilayers. Their study revealed a strong relationship between PL intensity and varying twist angles. Interestingly, bilayers twisted at random angles exhibited greater PL intensity compared to those twisted at 0° (AA stacking) and 60° (AB stacking). Using indirect-bandgap energy, or peak I, as a marker for interlayer electronic coupling strength, they illustrated the connection between the twist angle and the interlayer coupling strength. Furthermore, Liu et al. [75] found a similar trend in their study on MoS₂ bilayers, which helped consolidate the link between twist angles and PL intensity. All the bilayers observed displayed a significant drop in PL intensity compared to their monolayer counterparts. Interestingly, the bilayers with 0° and 60° twist angles, owing to their symmetric configuration, had the smallest indirect bandgap, suggesting the strongest interlayer coupling. Additionally, Wang et al.'s [63] research on WSe2/WS2 twisted heterostructure bilayers added another dimension to the understanding of interlayer coupling. They observed that post-annealing, the PL intensity of WS2 and WSe2 dropped dramatically, a strong indication of the formation of interlayer coupling. Collectively, these studies have highlighted the critical role of twist angles in the photonic properties of TMD bilayers, paving the way for promising applications in the field of photonics.

In the emerging field of t2DMs, moiré excitons have proven to be a pivotal phenomenon [152]. These excitons occur in layered TMD when a slight twist is introduced between the layers, creating a superlattice known as a moiré pattern [151]. This twist fundamentally alters the electronic band structure and gives rise to unique, strongly correlated phenomena including superconductivity, magnetism, and correlated insulating states [153]. Importantly, the moiré superlattice generates unique energy landscapes that localize and confine excitons, forming the moiré excitons. The properties of these excitons, such as their binding energies and spatial distributions, can be controlled by tuning the twist angle, thus offering unprecedented opportunities for exploring fundamental many-body quantum physics and designing innovative optoelectronic devices [145].

In 2019, an assortment of research groups unveiled the first experimental proof of moiré excitons present in TMD heterostructures. The studies revolved around various bilayer arrangements of TMD materials, encapsulated by hBN layers

[46,154–156]. Thanks to improved sample quality and the reduction of inhomogeneous linewidth, detailed structures of exciton resonances were discovered and linked to moiré mini bands. Tran et al. [155] conducted investigations on nearcommensurate structures and MoSe₂/WSe₂ hetero-bilayers (Figure 7(a) and (b)), a subject of two early studies. These research projects emphasized different spectroscopic attributes. They reported on multiple, comparatively broad interlayer excitons with around 10 meV linewidth. Two samples with twist angles approximately 1° and 2° were explored, as illustrated in Figure 7(c). Despite slight variations in peak energies, a larger resonance spacing was detected in the sample with a 2° twist angle. The resonances were ascribed to the ground and excited exciton states, trapped at a global minimum within the moiré supercell. The underlying explanation for these findings lies in the tighter lateral quantum confinement experienced by excitons in the smaller moiré supercell of the 2° sample, leading to a larger energy separation between the ground and excited states. The evidence supporting this interpretation is derived from the alternating circular polarization of the PL signal observed in the 1° sample, as depicted in Figure 7 (d). Concurrently, Seyler et al. [154] also examined MoSe₂/WSe₂ hetero-bilayers, but their focus centered on narrower resonances, with a linewidth of about 80 µeV (shown in Figure 7(i)). Such slender resonances were detected in hetero-bilayers with twist angles of approximately 2°, 57°, and 20°. It was inferred that all resonances in one sample stem from sites sharing the same interlayer atomic registry and C3 symmetry. In the same MoSe₂/ WSe₂ bilayers, more recent experiments have observed both narrow resonances and broader interlayer exciton resonances [157–160]. Bai et al. [161] observed a few sharp resonances and a broad peak that evolved into multiple, broader interlayer exciton resonances as excitation power increased, as shown in Figure 7(j). The sharp resonances were attributed to zerodimensional moiré potential traps, while the broader resonances were attributed to delocalized states.

New investigations indicated that these sharp resonances exhibit several characteristic traits of single-photon emitters [157,160]. Yet, the dominant trapping mechanism for excitons in these early spectroscopy experiments on TMD bilayers continues to be a subject of active debate [162]. In addition to the above, moiré excitons have been detected in incommensurate hetero-bilayers such as WS₂/ WSe₂ and WS₂/MoSe₂. Jin et al. [46] reported the division of an intralayer WSe₂ A exciton into multiple peaks in a WS₂/ WSe₂ hetero-bilayer (Figure 7(g) and (h)) with a twist angle smaller than 3°, as shown in Figure 7 (e). Contrarily, Zhang et al. [156] observed additional neutral exciton and trion resonances in a MoSe₂/MoS₂ hetero-bilayer with approximately a 1° twist angle (Figure 7(f)). Research on MoSe₂/WS₂

18 — Renlong Zhou et al. DE GRUYTER

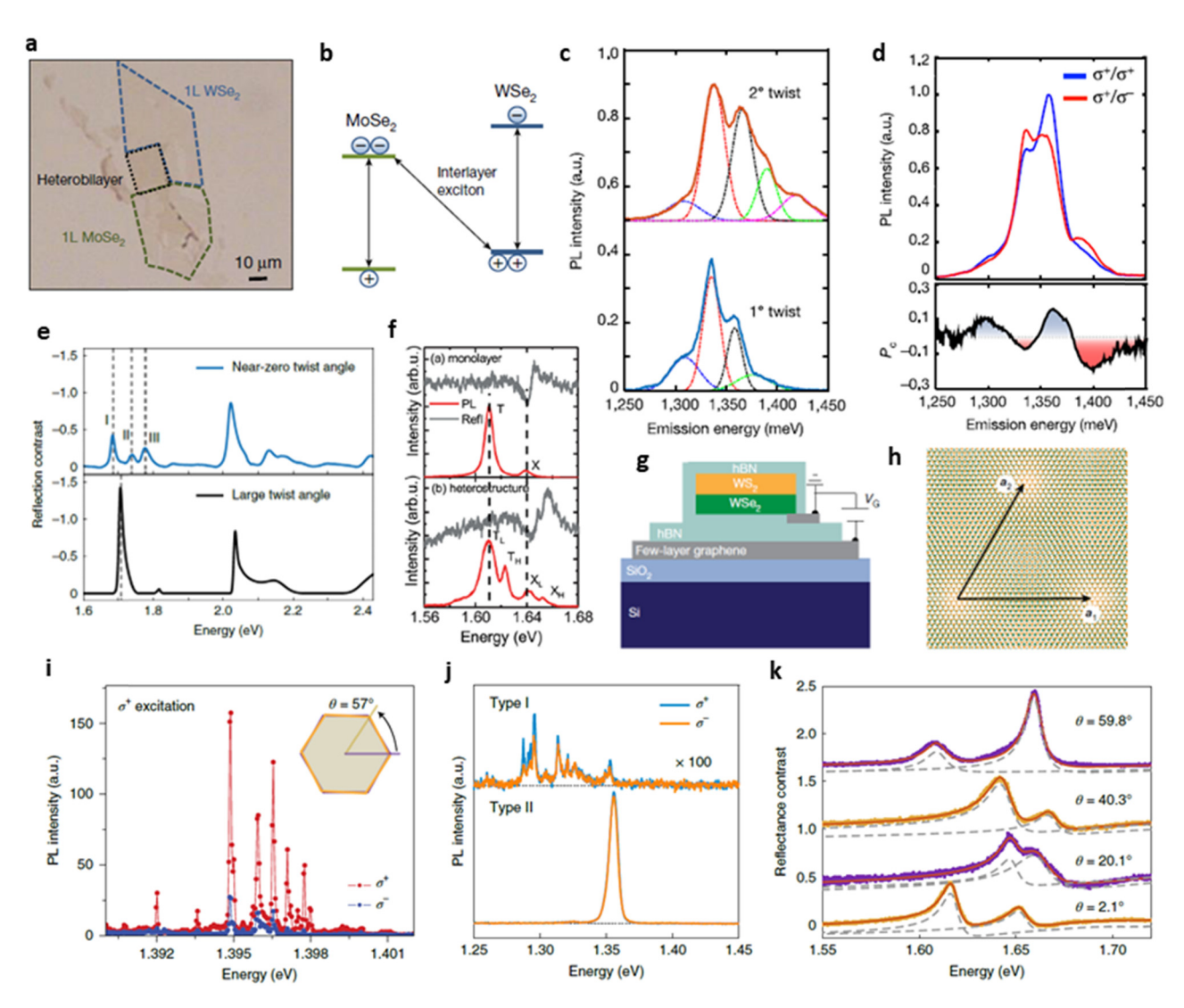


Figure 7: PL spectroscopy and moiré exciton phenomena within t2DMs. (a) It exhibits a visual representation of an hBN-covered MoSe₂/WSe₂ duallayered heterostructure, with the combined bilayer area enclosed by a black dashed circle. (b) A band blueprint is depicted, illuminating the type II alignment along with the interlayer exciton shift, denoted in arbitrary units. (c) Typical PL spectra are displayed for hetero-bilayers possessing 1° (bottom) and 2° (top) twist angles, each chart modeled with four (1°) or five (2°) Gaussian functions. (d) A circularly polarized PL spectrum corresponding to σ + excitation of the 1° sample is shown, with the degree of circular polarization illustrated against the emission wavelength in the lower section of the figure. (e) The reflective contrast spectrum of device D1 (displayed in light blue, top) is compared with that of a WSe₂/WS₂ heterostructure possessing a large twist angle (depicted in black, bottom). The latter demonstrates a sole resonance in the energy window 1.6-1.8 eV stemming from the WSe₂ A exciton state. However, the moiré superlattice generated in device D1 manifests three notable peaks of equal oscillator strength within this window (denoted I-III), signifying discrete moiré exciton states. (f) The PL and reflective spectra of a MoSe₂ monolayer and a MoS₂/MoSe₂ heterostructure are revealed. (g) and (h) A typical heterostructure with an almost zero twist angle is portrayed alongside a visual depiction of the moiré superlattice in real space, with the superlattice vectors, a1 and a2, stretching approximately 8 nm. (i) Pronounced interlayer exciton resonances and their helicity, observed in twisted MoSe₂/WSe₂ bilayers at lower excitation densities, are displayed. (j) Characteristic PL spectra from a pair of WSe₂/MoSe₂ hetero-bilayers show sharp resonances (type I) and a broad peak (type II), with right (σ +) and left (σ -) circularly polarized emission under σ + excitation signified by blue and orange spectra, respectively. The absence of circular emission in type II regions is ascribed to uniaxial strain. (k) Hybrid excitons within twisted MoSe₂/WS₂ bilayers are depicted, with individual hybrid exciton resonances demarcated by dashed lines. The figure is reproduced with the permission of (a)-(d) Ref. [155], © 2019 Nature Publishing Group, (e), (g), (h) Ref. [46], © 2019 Nature Publishing Group, (f) Ref. [156], © 2018 American Chemical Society, (i) Ref. [154], © 2019 Nature Publishing Group, (j) Ref. [161], © 2020 Nature Publishing Group, (k) Ref. [163], © 2020 Nature Publishing Group.

hetero-bilayers by Alexeev *et al.* [40] and Zhang *et al.* [163] identified the presence of hybrid excitons. In a series of samples, multiple resonances exhibiting systematic changes in energy splitting and relative intensity between the hybridized excitons were revealed, as demonstrated in Figure 7(k). This research has furthered the understanding of the interaction between intralayer and interlayer excitons in WSe₂/WS₂ and MoSe₂/WS₂ hetero-bilayers.

Indeed, the exploration of moiré excitons in TMD heterostructures is shaping up to be a fascinating field. There is a dynamic and active discourse happening around it, and the revelations so far are quite compelling, underlining the distinctive characteristics of these structures. As we continue to refine our experimental techniques and deepen our theoretical understanding, we anticipate even more enlightening discoveries. The implications of this research could potentially transform our current comprehension and manipulation of certain technologies. This is an intriguing voyage, and we eagerly await the upcoming revelations in this domain.

4 Device applications of t2DMs

4.1 Photodetection with t2DMs

The t2DMs have emerged as a fascinating platform for various optoelectronic applications, particularly in photodetectors. Their unique properties stem from the interlayer interactions and twist angles between atomically thin layers, which give rise to diverse electronic and optical characteristics [164]. In the realm of photodetectors, t2DM's flexibility and strong light-matter interaction set the stage for designing highly sensitive and responsive devices [163]. For example, heterostructures based on van der Waals materials such as TMDs can be engineered to create p-n junctions at an atomic level. By individually contacting layers of different materials, like p-type WSe₂ and n-type MoS₂, an atomically thin p-n junction is formed [165]. The difference in work function and bandgap between the layers creates an atomically sharp heterointerface with a predicted type II band alignment [165]. This fine control over the heterojunction properties enables gate-voltage-tuned rectification of current, leading to highly tunable photodetection capabilities. Furthermore, the strong light-matter interaction in TMDs and the availability of different bandgaps and work functions allow for bandgap engineering of heterostructures [166]. Such engineering facilitates the design of photodiodes, photovoltaic cells, and other light-emitting devices, which are fundamental in the development of efficient photodetectors. Additionally, the moiré patterns formed by the twist-induced superlattice in t2DM can modify the electronic band structure, enhancing light absorption across a wide range of wavelengths. This enhancement in light absorption can lead to an improvement in the efficiency of photodetectors by promoting the generation of electron—hole pairs [167,168].

When the incident photon's energy aligns with the energy difference in the material, an augmented photoresponse can be created. Utilizing this concept, Yin et al. [169] and Tan et al. [170] pioneered the use of CVD-tBLG for photodetection in 2016. They cultivated tBLG with varying twist angles on copper substrates, ultimately selecting unique samples with 13° and 10.5° twist angles. These were then transferred to a heavily doped Si substrate with a 90 nm SiO₂ layer for device assembly. The structure of the device is shown in Figure 8(a), and the experimental findings showed that different samples were sensitive to distinct wavelength regions, a result consistent with prior photo-absorption theories. Through this photodetector, they achieved a remarkable 6.6-fold enhancement in photocurrent. By synergizing with metal plasmon nanostructures, they further amplified the photo-response by approximately 80 times (Figure 8(b)). Besides the enhanced photocurrent response, Raman mapping further illustrated the pronounced signal within the twisted regions, as depicted in Figure 8(c) and (d). This observation highlights the intricate interplay between the structural properties of the twisted regions and their corresponding optical characteristics. The strong Raman signal in the twisted area may offer additional insights into the unique electronic and optical behavior exhibited by these structures, indicating potential pathways for tuning and optimization in photodetection applications.

Around the same time, comparable outcomes were published by other research teams. Chen et al. [82] initially evaluated the photo-response of tBLG samples in a TIR mode, observing a substantial polarization-dependent photocurrent, most prominent at the gold electrodes and graphene interface (Figure 8(e)). Subsequently, Xin et al. [171] conducted an in-depth exploration using a conventional Kretschmann configuration system. They fabricated various graphene samples, including monolayer, bilayer, trilayer, and tBLG with 10.0° and 12.0° angles and employed them as light-harvesting materials in a typical metal-graphene-metal photodetector architecture. Their meticulous comparison revealed that the robust interlayer coupling in tBLG, rather than the sheer thickness of the material, had a more significant influence on the enhancement of photoresponse. Furthermore, by applying Maxwell's equations in a multilayer material model, they ascertained that the 20 — Renlong Zhou et al. DE GRUYTER

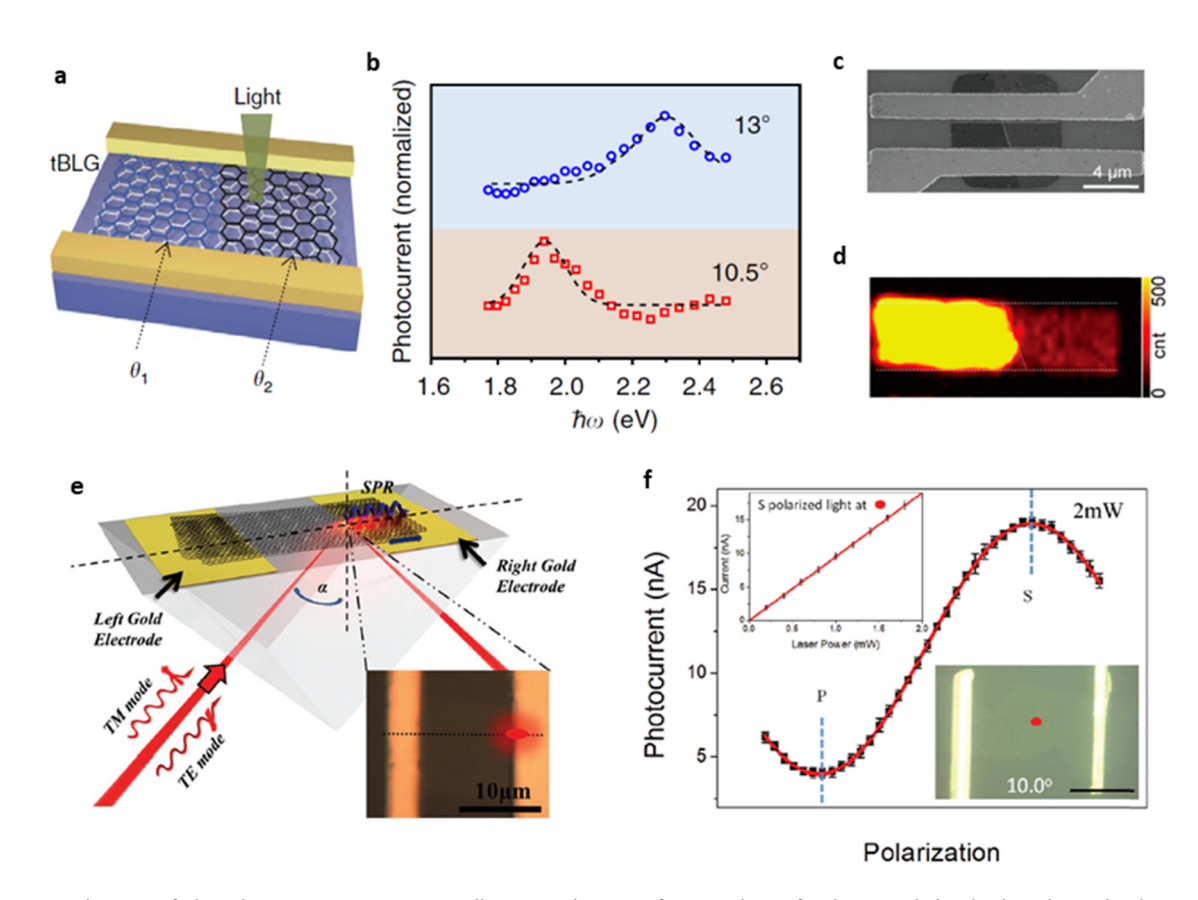


Figure 8: Exploration of photodetection in t2DMs. (a) An illustrative diagram of a tBLG device for detecting light; (b) the relationship between photocurrent and photon energy across various tBLG structures; (c) an SEM view of the tBLG photodetector, illustrating a twist angle of roughly 10°, with the bilayer section located to the left of a marked line and the monolayer to the right; (d) a visualization through Raman G-band mapping, activated by a 633 nm laser; (e) a representation of the configuration used to measure tBLG photovoltage in TIR mode; and (f) a description of how the tBLG photodetector responds to different polarization states in TIR mode, including an inset that depicts how photocurrent varies with the intensity of the incident light. The figure is reproduced with the permission of (a) and (b) Ref. [169], © 2016 Nature Publishing Group, (c) and (d) Ref. [170], © 2016 American Chemical Society, (e) and (f) Ref. [148], © 2016 Wiley-VCH.

gold electrode's surface plasmon resonance contributed to the polarization-dependent traits of the device. This led to a photo-response in the transverse magnetic (TM) mode that was around 1.8 times greater than that in the transverse electric (TE) mode. Utilizing the device in TIR mode, they realized a sevenfold increase in photovoltage. Figure 8(f) provides a schematic depiction of the sample's structure, alongside the polarization-dependent photo-response, and the simulated photo-absorption for both TM and TE incident light. This illustration offers a comprehensive view of how the twisted structure interacts with light of different polarizations, presenting a detailed comparison of the absorption characteristics for TM and TE modes.

The applications of t2DMs in photodetectors are vast and hold great promise for the future of optoelectronics. Their unique properties, such as the ability to create high-quality heterointerfaces without atomic-level precision, and the strong light-matter interaction, make t2DMs a

versatile and promising candidate for designing next-generation photodetectors. The ongoing research and technological advancements in this area are likely to unlock new potential in various fields including telecommunications, medical imaging, and environmental monitoring.

4.2 Single-photon detector and interlayer exciton laser

The capability to detect light at the level of individual photons has immense implications across a range of fields, from quantum computing and sensing to security through quantum key distribution and even applications in radio astronomy [172]. Traditional approaches to single-photon detectors have leveraged the interruption of superconducting states within nanostructured superconductors.

This approach has successfully led to commercialized detectors that function within visible to near-IR wavelengths. However, the high electron density and resultant large heat capacity of standard superconductors have historically posed challenges for detection in ultralow photon energy regions, such as mid-IR and terahertz frequencies. Remarkably, magic-angle tBLG moiré superlattices have been shown to offer a solution to this problem [37]. These structures can exhibit superconducting states at an extraordinarily low electron density, around 10^{12} cm⁻², which translates into a minimal heat capacity, on the order of a few hundred times the Boltzmann constant [173,174] (Figure 9(e)). As a result, even a single photon of very low energy is sufficient to cause a significant temperature increase, breaking down the superconducting state. This has opened up new opportunities for single-photon detection in areas previously thought unreachable, including the mid-IR and terahertz range [37,173,174] (Figure 9(c)).

Theoretical models have illustrated that magic-angle tBLG can provide a single-photon detection range that

extends from the visible spectrum to sub-terahertz, boasting a remarkable response time of around 4 ns and an energy resolution better than 1 THz [173]. These exciting possibilities are not yet realized in practice, and further experimental work is needed to bring such groundbreaking single-photon devices into existence [175,176]. Beyond these promising detection capabilities, the unique characteristics of moiré superlattices may also lead to other enhancements in optoelectronic properties. Integration with various structures such as waveguides, cavities, plasmonic, and ring resonators could enable a vast array of innovative optoelectronic devices, such as single-photon light-emitting devices, optical modulators, and photo-induced valley currents. The exploration of these avenues has the potential to significantly advance the field of photonics, capitalizing on the unique properties of t2DMs.

Interlayer exciton lasers based on t2DMs are an emerging area of research that leverages the novel physical properties of these materials to produce lasers with

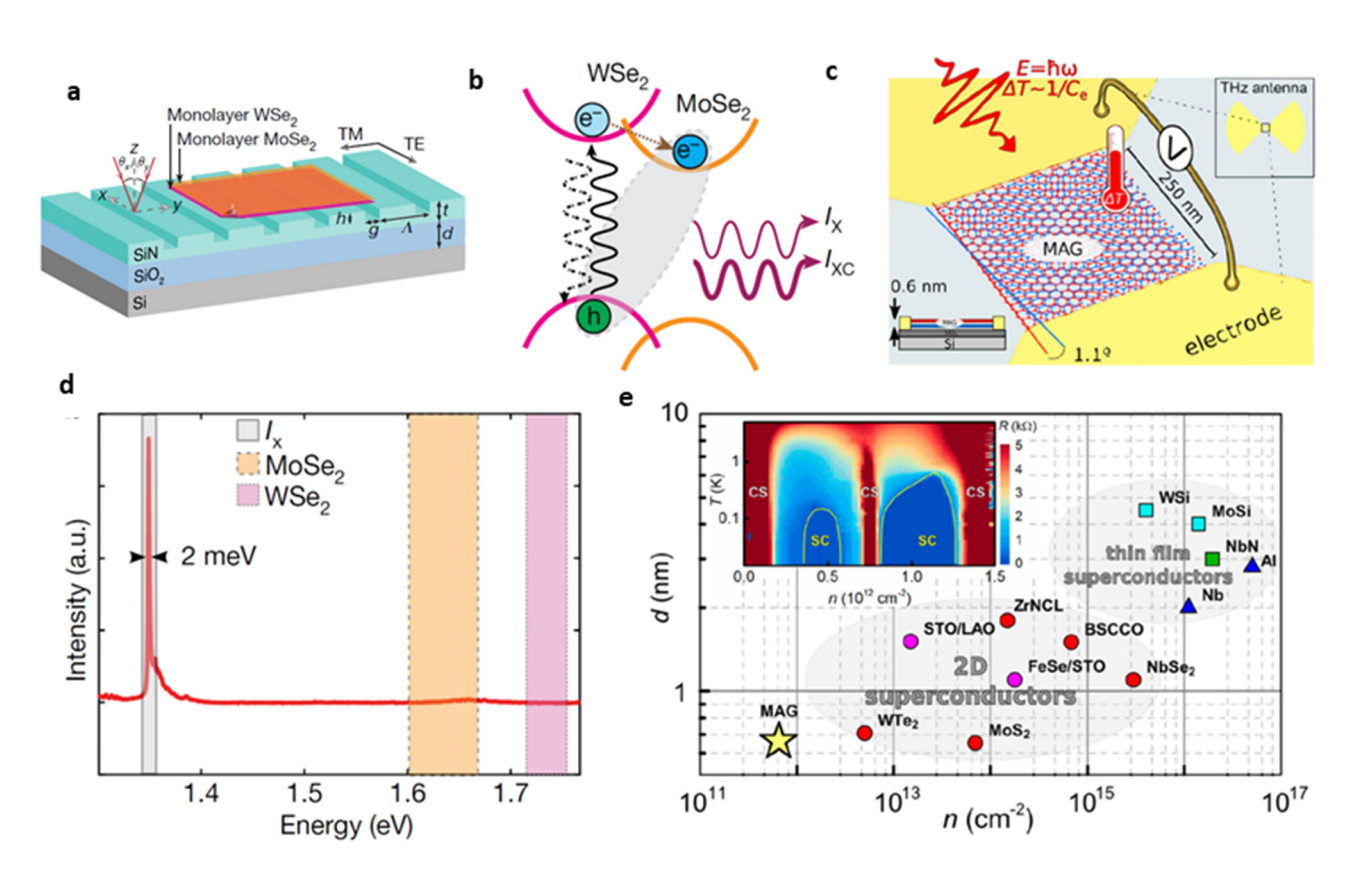


Figure 9: Interlayer exciton laser and single-photon detector. (a) The schematic diagram of the WSe₂/MoSe₂ interlayer exciton laser device. (b) IThe band alignment and carrier dynamics of the hetero-bilayer, emphasizing the type II band alignment and forming a three-level system for the injected carriers, and the excitement of intralayer excitons in the WSe₂ layer by a pump laser. (c) The schematic cartoon of magic-angle tBLG superconducting single-photon nanocalorimeter. (d) The PL spectrum from the hetero-bilayer, pumped with a 633-nm laser at 20 μ W, highlighting the spectral range of interlayer (IX), MoSe₂, and WSe₂ exciton emission. (e) The carrier density and thickness between superconductor magic-angle tBLG and 2D thin film superconductors below 10 nm, with an inset offering a glimpse of the phase diagram of magic-angle tBLG. The figure is reproduced with the permission of (a), (b), (d) Ref. [177], © 2019 Nature Publishing Group, (c) and (e) Ref. [173], © 2020 American Chemical Society.

potentially groundbreaking capabilities [178]. In typical semiconductor materials, excitons are formed by the electrostatic attraction between electrons and holes. In t2DMs, the unique stacking and twisting of layers can give rise to what is known as interlayer excitons, where electrons and holes reside in different layers of the structure [172]. This spatial separation of charge carriers leads to long-lived excitonic states due to reduced recombination rates. An extraordinary advancement in the utilization of interlayer excitons was recently achieved in a study by Paik et al. [177]. They managed to harness the robust coupling of interlayer excitons by crafting an exciton laser, a feat achieved by integrating a WSe₂/MoSe₂ hetero-bilayer into a silicon nitride (Si₃N₄) grating resonator. This innovation led to the creation of a laser exhibiting exceptional spatial and temporal coherence (see Figure 9(a) for the device's schematic design). Utilizing a hetero-bilayer WSe₂/MoSe₂ with a precise 0° interlayer twist angle as the gain medium, they succeeded in realizing population inversion density under minimal excitation (633 nm, 20 μW), leading to pronounced exciton emission as seen in PL measurements. The type II band alignment was pinpointed as an influential factor in this process (illustrated in Figure 9(b)). The work not only lays a substantial foundation but also opens exciting avenues for future explorations in this field.

4.3 LED and ultrafast modulators

Twisted van der Waals (vdW) materials exhibit unique optoelectronic properties that make them promising candidates for light-emitting diode (LED) applications [94]. The moiré superlattice formed by the twisted layers can modulate the electronic band structure, leading to enhanced light emission [179]. The twist angle can be tuned to control the exciton binding energy and emission wavelength, enabling the design of efficient light sources across a wide spectral range. Additionally, the strong light–matter interactions in tTMDs can lead to enhanced spontaneous emission rates, further improving LED performance [180].

In the ultrafast regime, twisted vdW materials exhibit unique carrier dynamics due to the moiré superlattice potential [181]. The periodic modulation of the band structure can lead to ultrafast charge transfer and separation, enabling applications in ultrafast optoelectronics and photonics. The twist angle can be used to engineer the carrier dynamics, allowing for precise control over the ultrafast response [180]. These properties make twisted vdW materials suitable for ultrafast modulators, essential components in optoelectronic devices where they control the intensity,

phase, polarization, or propagation direction of light with high precision [182]. The tunability offered by the twist angle allows for the development of modulators that operate at unprecedented speed and efficiency.

5 Challenges and future perspectives

5.1 Integration with other photonic materials and systems

Incorporating twisted layered materials with other photonic substances and systems can pave the way for heightened functionalities and groundbreaking device frameworks. The unique properties and tunability of t2DMs can be synergistically combined with various photonic materials and systems to achieve advanced photonic devices and systems. One approach is to integrate twisted layered materials with plasmonic structures. Plasmonic materials, such as gold or silver nanoparticles, can provide strong field confinement and enhance light-matter interactions [183]. By combining t2DMs with plasmonic structures, it is possible to achieve enhanced light absorption, emission, and manipulation. For example, the plasmonic resonance can be tuned by the twist angle, enabling control over the plasmonic response of the integrated system. This integration can lead to the development of high-performance sensors, photodetectors, and enhanced light-emitting devices [184].

Additionally, twisted layered materials can be integrated into photonic crystal structures. Photonic crystals are periodic structures that exhibit bandgaps and control the flow of light [185]. By incorporating t2DMs into the photonic crystal lattice, it is possible to achieve tunable bandgaps and modify the dispersion properties of photons. This integration can enable efficient light routing, waveguiding, and selective filtering. Moreover, the combination of twisted layered materials and photonic crystals can lead to the development of compact and highly efficient optical devices, such as on-chip lasers, modulators, and sensors.

Integration with traditional semiconductor-based photonic systems is another avenue for exploiting the potential of twisted layered materials. By incorporating t2DMs into semiconductor optical devices, such as waveguides, photodetectors, or light-emitting diodes, it is possible to enhance their performance and functionalities. The twist-induced changes in the band structure, excitonic properties, and light-matter interactions can be harnessed to achieve improved device efficiency, reduced energy consumption, and novel functionalities [186].

Furthermore, twisted layered materials can be integrated into fiber optic systems. By coating or embedding t2DMs onto optical fibers, it is possible to achieve active and tunable modulation of light signals. This integration can enable dynamic control over the fiber transmission properties, such as attenuation, dispersion, or polarization. It can also lead to the development of reconfigurable fiber optic devices and systems for applications in telecommunications, data transmission, and sensing. The integration of t2DMs with other photonic materials and systems offers a rich landscape of opportunities for advanced photonic devices and systems. The unique properties, tunability, and compatibility of t2DMs with various photonic platforms pave the way for innovative applications in sensing, communication, imaging, and optoelectronics. Continued research and development in this field will further expand the potential of integrated photonic systems based on t2DMs.

5.2 Exploration of novel optical phenomena in t2DMs

The exploration of novel optical phenomena in twisted layered materials has emerged as a fascinating area of research. The unique structural and electronic properties of t2DMs, arising from the interlayer coupling and moiré patterns, give rise to intriguing optical phenomena that are not present in their individual constituent layers or bulk counterparts. These phenomena provide insights into fundamental physics and open up new possibilities for the development of advanced photonic devices and systems. One of the remarkable optical phenomena observed in twisted layered materials is the emergence of new electronic states and interlayer excitons. The moiré superlattice formed by the lattice mismatch between the layers introduces a periodic potential landscape, modifying the electronic band structure [187,188]. This leads to the formation of minibands, flatbands, and van Hove singularities in the electronic density of states. These unique electronic states give rise to novel optical transitions, including twistinduced interlayer excitons with enhanced binding energies and long lifetimes. The exploration of these interlayer excitons has unveiled interesting optical properties such as strong light-matter interactions, unconventional PL spectra, and efficient energy transfer processes.

Moreover, t2DMs exhibit intriguing nonlinear optical phenomena. The nonlinear optical response in t2DMs can be enhanced due to the long exciton lifetimes, large exciton binding energies, and unique band structures. Nonlinear effects such as SHG, THG, and four-wave mixing have been

observed in t2DMs. The twist-induced modulation of the nonlinear optical response offers opportunities for efficient nonlinear frequency conversion, ultrafast optical modulation, and nonlinear optical signal processing. Another fascinating optical phenomenon in twisted layered materials is the manifestation of topological states [189]. The interplay between the twist angle and the material's intrinsic spin-orbit coupling can give rise to topological phases with protected edge states. The twisted structure introduces a synthetic gauge field that modifies the electronic dispersion and leads to the formation of topological bands [190-193]. This opens possibilities for exploring topological effects, such as topologically protected photonic modes, valleytronics, and quantum Hall-like phenomena, in t2DMs [145]. Additionally, twisted layered materials exhibit unique optical response due to their anisotropic properties. The moiré patterns introduce spatially varying optical properties, including polarizationdependent absorption, reflection, and transmission. This anisotropy can be utilized for controlling and manipulating light polarization, enabling polarization-sensitive devices and applications. Furthermore, the twist angle-dependent optical response enables tunable optical properties, including wavelength-selective absorption and emission, tunable photonic bandgaps, and dynamic control over light transmission characteristics. The exploration of these novel optical phenomena in twisted layered materials not only enhances our understanding of fundamental physics but also offers opportunities for developing advanced photonic devices. The manipulation of twist angle, material choice, and device design enables the tailoring of optical properties and functionalities. Continued research in this field aims to further uncover and harness these optical phenomena for applications in areas such as optics, optoelectronics, quantum technologies, and energy harvesting.

5.3 Characterization techniques

Improving characterization techniques is essential for advancing the understanding and application of t2DMs. Current methods, based on far-field techniques, often yield complex and convoluted results due to the involvement of thousands of moiré unit cells. To overcome this challenge and gain deeper insights, it is imperative to develop techniques capable of probing individual supercells with ultrahigh resolution. Techniques such as near-field scanning optical microscopy, STM tip-induced luminescence, and cathodoluminescence (CL) imaging hold significant potential for achieving this level of precision. Enhanced characterization methods will enable simultaneous imaging of supercells, assessment of the moiré potential, and characterization of correlated states

through optical spectroscopy measurements. By achieving this level of precision, it becomes possible to resolve existing mysteries and shed light on unresolved questions, thereby propelling further advancements in the field.

5.4 External manipulation of properties

Manipulating the photonic and optoelectronic properties of t2DMs through external factors offers significant potential for new functionalities and applications. The application of an electric field can modify the overall moiré potential minima due to distinct local static dipole moments. Similarly, strain can reshape the moiré potential landscape and impact the optoelectronic response, while light can influence spin-spin interactions, offering the potential for all-optical control of emergent phenomena. Understanding and controlling these interactions can lead to novel functionalities such as quantum nonlinear optics, laser technologies, imaging arrays, modulation and switching devices, and polarization devices. These manipulations open new horizons for research and development in twisto-photonics, providing versatile tools for tuning material properties and enhancing device performance.

5.5 Theoretical modeling and simulation

Accurate theoretical modeling and simulation of t2DMs present significant challenges due to the complex interplay between electronic, optical, and mechanical properties. Advanced computational methods are required to predict the behavior of these materials accurately and guide experimental efforts. These models must account for various factors, including strain, electronic interactions, and environmental conditions, to provide reliable predictions that can be validated experimentally. Additionally, developing models that can simulate the effects of external manipulation, such as electric fields and strain, will be crucial for designing and optimizing new devices. Theoretical insights can also help in understanding the fundamental physics underlying the observed phenomena in twisto-photonics, thereby driving further innovation and discovery in the field.

5.6 Development of scalable fabrication techniques

The development of scalable fabrication techniques for t2DMs presents a complex challenge that involves a multi-

faceted approach. Precise control over the twist angle is paramount, as even slight variations can dramatically change the properties of t2DMs, yet achieving this control consistently across large areas is intricate and demands advanced methods. The delicate nature of handling and manipulating thin 2D layers adds to the complexity, making the scaling process from lab to industrial production a difficult task. Integration with existing manufacturing workflows poses a unique set of obstacles due to compatibility and specific handling requirements of these materials. Challenges also stem from material and substrate compatibility, which may limit scalability and high costs associated with new equipment and process development. Quality control is vital, and devising real-time measures to ensure consistency across large production runs is an ongoing effort. Further, the time- and labor-intensive nature of many current fabrication methods necessitates innovative solutions to become economically viable for mass production. Environmental sensitivity to factors like humidity and temperature, as well as technical challenges in hybrid integration and functionalization, contribute to the intricacy of scaling fabrication techniques. Together, these factors underline the multifarious challenges in developing scalable fabrication processes for t2DM, a focus area that holds the key to unlocking their full potential in diverse applications such as photonics, electronics, and sensing.

5.7 Technological and commercial prospects of twisted layered materials

Twisted layered materials hold tremendous technological and commercial prospects across a range of fields, driven by their unique properties and potential applications. In terms of technology, one of the most promising areas is the development of novel optoelectronic devices. Twisted structures offer opportunities to design photodetectors, light-emitting diodes, photovoltaics, and optical modulators with enhanced functionalities. The ability to tune the optical and electronic properties, including the emergence of interlayer excitons and moiré-induced effects, can result in devices with improved performance, efficiency, and tunability compared to conventional counterparts. Another exciting prospect lies in the realm of quantum technologies. The emergence of moiréinduced flat bands and topological phases in twisted layered materials opens doors for exploring quantum phenomena and applications. Twisted structures serve as platforms for studying quantum Hall effects, fractional quantum Hall states, and other exotic quantum phenomena. Additionally, the long coherence times of interlayer excitons make twisted layered

materials promising candidates for quantum information processing and quantum communication applications.

Energy harvesting and storage also benefit from the prospects offered by twisted layered materials. By leveraging the unique electronic and optical properties in conjunction with scalable fabrication techniques, it is possible to develop efficient energy harvesting devices, such as solar cells and thermoelectric generators. Furthermore, twisted layered materials can be explored for energy storage applications, including supercapacitors and batteries, by utilizing their large surface area and tunable electrochemical properties. Sensors and detectors represent another area of opportunity. The exceptional sensitivity of twisted layered materials to external stimuli, such as strain, electric fields, and gases, makes them attractive for sensing applications. Integrating twisted layered materials into sensor platforms enables high sensitivity, selectivity, and response times for various applications, including environmental monitoring, biomedical sensing, and chemical detection.

6 Conclusion

In conclusion, this article is a detailed guide through the quickly evolving field of photonics involving t2DMs, spotlighting the critical breakthroughs and innovative work steering this dynamic area of study. We delve deeply into the methods of fabricating these materials, notably highlighting the widely utilized one-step CVD process and the stacking method, while outlining their respective challenges and successes. The cornerstone of the article is the exploration of the photonic properties of these materials, where we unravel a range of intricate phenomena including optical absorption, plasmonic, and chirality, casting a special focus on the captivating area of moiré excitons and technologies like Raman spectroscopy and PL used to study them. Moving forward, we present the latest in device applications, offering readers a deep understanding of recent advancements in photodetection technologies and venturing into new areas like single-photon detectors and interlayer exciton lasers. As we look towards the future, we discuss the exciting potential for integration with other photonic materials, opening doors to discovering unprecedented optical phenomena in t2DMs. This article aims to be a beacon, encouraging researchers to explore this promising terrain and underlining the substantial role these materials will play in the forward-moving field of photonics, ushering in a future rich with new functionalities and revolutionary progress.

Funding information: The authors acknowledge the support provided by the Guangdong Basic and Applied Basic

Research Foundation (2020A1515110488) and the Scientific Key Research Fund of Guangdong Provincial Education Department (2019KZDXM061, 2019KQNCX099, 2020ZDZX2059, 2021ZDZX1038).

Author contributions: All authors have accepted responsibility for the entire content of this manuscript and approved its submission.

Conflict of interest: The authors state no conflict of interest.

Data availability statement: All data generated or analyzed in this study are included in this published article.

References

- [1] Novoselov KS, Geim AK, Morozov SV, Jiang D, Zhang Y, Dubonos SV, et al. Electric field effect in atomically thin carbon films. Science. 2004;306:666–9.
- [2] Geim AK, Novoselov KS. The rise of graphene. Nat Mater. 2007;6:183–91.
- [3] Guo B, Lan Xiao Q, Hao Wang S, Zhang H. 2D layered Materials: Synthesis, nonlinear optical properties, and device applications. Laser Photon Rev. 2019;13:1–46.
- [4] You JW, Bongu SR, Bao Q, Panoiu NC. Nonlinear optical properties and applications of 2D materials: Theoretical and experimental aspects. Nanophotonics. 2018;8:63–97.
- [5] Schaibley JR, Yu H, Clark G, Rivera P, Ross JS, Seyler KL, et al. Valleytronics in 2D materials. Nat Rev Mater. 2016;1:1–15.
- [6] Castro Neto AH, Guinea F, Peres NMR, Novoselov KS, Geim AK. The electronic properties of graphene. Rev Mod Phys. 2009;81:109–62.
- [7] Luo S, Wang Y, Tong X, Wang Z. Graphene-based optical modulators. Nanoscale Res Lett. 2015;10:1–11.
- [8] Xu M, Liang T, Shi M, Chen H. Graphene-like two-dimensional materials. Chem Rev. 2013;113:3766–98.
- [9] Mak KF, Lee C, Hone J, Shan J, Heinz TF. Atomically thin MoS₂: a new direct-gap semiconductor. Phys Rev Lett. 2010;105:136805.
- [10] Krasnok A, Alù A. Valley-selective response of nanostructures coupled to 2D transition-metal dichalcogenides. Appl Sci. 2018;8:1157.
- [11] Xiao J, Ye Z, Wang Y, Zhu H, Wang Y, Zhang X. Nonlinear optical selection rule based on valley-exciton locking in monolayer WS2. Light Sci Appl. 2015;4:e366.
- [12] Dean CR, Young AF, Meric I, Lee C, Wang L, Sorgenfrei S, et al. Boron nitride substrates for high-quality graphene electronics. Nat Nanotechnol. 2010;5:722–6.
- [13] Caldwell JD, Aharonovich I, Cassabois G, Edgar JH, Gil B, Basov DN. Photonics with hexagonal boron nitride. Nat Rev Mater. 2019;4:552–67.
- [14] Futaba DN. Hexagonal boron nitride heterostructures go large. Nat Electron. 2023;6:104–5.
- [15] Su C, Zhang F, Kahn S, Shevitski B, Jiang J, Dai C, et al. Tuning colour centres at a twisted hexagonal boron nitride interface. Nat Mater. 2022;21:896–902.

- [16] King A, Johnson G, Engelberg D, Ludwig W, Marrow J. Observations of intergranular stress corrosion cracking in a grain-mapped polycrystal. Science. 2008;321:382–5.
- [17] Kim KS, Zhao Y, Jang H, Lee SY, Kim JM, Kim KS, et al. Large-scale pattern growth of graphene films for stretchable transparent electrodes. Nature. 2009;457:706–10.
- [18] Novoselov KS, Jiang D, Schedin F, Booth TJ, Khotkevich VV, Morozov SV, et al. Two-dimensional atomic crystals. Proc Natl Acad Sci USA. 2005;102:10451–3.
- [19] Han X, Zhao C, Wang S, Pan Z, Jiang Z, Tang X. Multifunctional TiO₂/C nanosheets derived from 3D metal -organic frameworks for mild-temperature-photothermal-sonodynamic-chemodynamic therapy under photoacoustic image guidance. J Colloid Interface Sci. 2022:621:360–73.
- [20] Bistritzer R, MacDonald AH. Moiré bands in twisted double-layer graphene. Proc Natl Acad Sci USA. 2011;108:12233–7.
- [21] Xiao D, Bin Liu G, Feng W, Xu X, Yao W. Phys Rev Lett. 2012;108.
- [22] Schreppler S, Spethmann N, Brahms N, Botter T, Barrios M, Stamper-Kurn DM. Optically measuring force near the standard quantum limit. Science. 1979;2014(344):1486–9.
- [23] Hunt B, Sanchez-Yamagishi JD, Young AF, Yankowitz M, Leroy BJ, Watanabe K, et al. Massive dirac fermions and hofstadter butterfly in a van der waals heterostructure. Science. 2013;340:1427–30.
- [24] Esaki L, Tsu R. Superlattice and negative differential conductivity in semiconductors. IBM | Res Dev. 1970;14:61–5.
- [25] Steele W. Monolayer adsorption with lateral interaction on heterogeneous surfaces. J Phys Chem. 1963;67:2016–23.
- [26] Dean CR, Young AF, Meric I, Lee C, Wang L, et al. Boron nitride substrates for high-quality graphene electronics. Nat Nanotechnol. 2010;5:722–26.
- [27] Patil C, Dalir H, Kang JH, Davydov A, Wong CW, Sorger VJ. Highly accurate, reliable, and non-contaminating two-dimensional material transfer system. Appl Phys Rev. 2022;9:011419.
- [28] Schranghamer TF, Sharma M, Singh R, Das S. Review and comparison of layer transfer methods for two-dimensional materials for emerging applications. Chem Soc Rev. 2021;50:11032–54.
- [29] Watson AJ, Lu W, Guimaraes MHD, Stöhr M. Transfer of largescale two-dimensional semiconductors: Challenges and developments. 2D Mater. 2021;8:032001.
- [30] Shen C, Chu Y, Wu QS, Li N, Wang S, Zhao Y, et al. Correlated states in twisted double bilayer graphene. Nat Phys. 2020:16:520–5.
- [31] Yang F, Song W, Meng F, Luo F, Lou S, Lin S, et al. Tunable second harmonic generation in twisted bilayer graphene. Matter. 2020;3:1361–76.
- [32] Cheng Y, Huang C, Hong H, Zhao Z, Liu K. Emerging properties of two-dimensional twisted bilayer materials. Chin Phys B. 2019;28:107304.
- [33] Cai L, Yu G. Fabrication strategies of twisted bilayer graphenes and their unique properties. Adv Mater. 2021;33:1–24.
- [34] Gao X-GG, Li X-KK, Xin W, Chen X-DD, Liu Z-BB, Tian J-GG. Fabrication, optical properties, and applications of twisted twodimensional materials. Nanophotonics. 2020;9:1717–42.
- [35] Tang B, Che B, Xu M, Ang ZP, Di J, Gao H-J, et al. Recent advances in synthesis and study of 2D twisted transition metal dichalcogenide bilayers. Small Struct. 2021;2:2000153.
- [36] Nimbalkar A, Kim H. Opportunities and challenges in twisted bilayer graphene: a review. Nanomicro Lett. 2020;12:1–20.

- [37] Cao Y, Fatemi V, Fang S, Watanabe K, Taniguchi T, Kaxiras E, et al. Unconventional superconductivity in magic-angle graphene superlattices. Nature. 2018;556:43.
- [38] Liu E, Barré E, van Baren J, Wilson M, Taniguchi T, Watanabe K, et al. Signatures of moiré trions in WSe₂/MoSe₂ heterobilayers. Nature. 2021;594:46.
- [39] Chen G, Sharpe AL, Fox EJ, Zhang YH, Wang S, Jiang L, et al. Tunable correlated chern insulator and ferromagnetism in a moiré superlattice. Nature. 2020;579:56.
- [40] Alexeev EM, Ruiz-Tijerina DA, Danovich M, Hamer MJ, Terry DJ, Nayak PK, et al. Resonantly hybridized excitons in moiré superlattices in van der waals heterostructures. Nature. 2019;567:81.
- [41] Cao Y, Fatemi V, Demir A, Fang S, Tomarken SL, Luo JY, et al. Correlated insulator behaviour at half-filling in magic-angle graphene superlattices. Nature. 2018;556:80.
- [42] Zhang L, Wu F, Hou S, Zhang Z, Chou YH, Watanabe K, et al. Van der waals heterostructure polaritons with moiré-induced nonlinearity. Nature. 2021;591:61.
- [43] Yang W, Chen G, Shi Z, Liu CC, Zhang L, Xie G, et al. Epitaxial growth of single-domain graphene on hexagonal boron nitride. Nat Mater. 2013;12:792.
- [44] Hu Q, Zhan Z, Cui H, Zhang Y, Jin F, Zhao X, et al. Observation of Rydberg moiré excitons. Science. 1979;2023(380):1367.
- [45] Ponomarenko LA, Gorbachev RV, Yu GL, Elias DC, Jalil R, Patel AA, et al. Cloning of dirac fermions in graphene superlattices. Nature. 2013;497:594.
- [46] Jin C, Regan EC, Yan A, Iqbal Bakti Utama M, Wang D, Zhao S, et al. Observation of moiré excitons in WSe₂/WS₂ heterostructure superlattices. Nature. 2019;567:76.
- [47] Sharpe AL, Fox EJ, Barnard AW, Finney J, Watanabe K, Taniguchi T, et al. Emergent ferromagnetism near three-quarters filling in twisted bilayer graphene. Science (1979). 2019;365:605.
- [48] Hsu WT, Zhao ZA, Li LJ, Chen CH, Chiu MH, Chang PS, et al. Second harmonic generation from artificially stacked transition metal dichalcogenide twisted bilayers. ACS Nano. 2014;8:2951.
- [49] Hu G, Ou Q, Si G, Wu Y, Wu J, Dai Z, et al. Topological polaritons and photonic magic angles in twisted α-MoO₃ bilayers. Nature.
- [50] Huang T, Tu X, Shen C, Zheng B, Wang J, Wang H, et al. Observation of chiral and slow plasmons in twisted bilayer graphene. Nature. 2022;605:63.
- [51] Wang H, Wang S, Zhang S, Zhu M, Ouyang W, Li Q. Deducing the internal interfaces of twisted multilayer graphene via moiréregulated surface conductivity. Natl Sci Rev. 2023;10(8):nwad 175.
- [52] Xian L, Kennes DM, Tancogne-Dejean N, Altarelli M, Rubio A. Multiflat bands and strong correlations in twisted bilayer boron nitride: Doping-induced correlated insulator and superconductor. Nano Lett. 2019;19:4934.
- [53] Nguyen VH, Hoang TX, Charlier JC. Electronic properties of twisted multilayer graphene. J Phys Mater. 2022;5:034003.
- [54] Robinson JT, Schmucker SW, Diaconescu CB, Long JP, Culbertson JC, Ohta T, et al. Electronic hybridization of large-area stacked graphene films. ACS Nano. 2013;7:637.
- [55] Kim K, DaSilva A, Huang S, Fallahazad B, Larentis S, Taniguchi T, et al. Tunable moiré bands and strong correlations in smalltwist-angle bilayer graphene. Proc Natl Acad Sci USA. 2017:114:3364
- [56] Ribeiro-Palau R, Zhang C, Watanabe K, Taniguchi T, Hone J, Dean CR. Twistable electronics with dynamically rotatable heterostructures. Science. 2018;361:690–3.

DE GRUYTER

- [58] Cao Y, Luo JY, Fatemi V, Fang S, Sanchez-Yamagishi JD, Watanabe K, et al. Superlattice-induced insulating states and valley-protected orbits in twisted bilayer graphene. Phys Rev Lett. 2016;117:116804.
- Lui CH, Ye Z, Ji C, Chiu KC, Chou CT, Andersen TI, et al. Observation of interlayer phonon modes in van der Waals heterostructures. Phys Rev B Condens Matter Mater Phys. 2015;91:165403.
- Huang S, Ling X, Liang L, Kong J, Terrones H, Meunier V, et al. Probing the interlayer coupling of twisted bilayer MoS₂ using photoluminescence spectroscopy. Nano Lett. 2014;14:5500.
- Liao M, Wei Z, Du L, Wang Q, Tang J, Yu H, et al. Precise control of the interlayer twist angle in large scale MoS₂ homostructures. Nat Commun. 2020;11:2153.
- Puretzky AA, Liang L, Li X, Xiao K, Sumpter BG, Meunier V, et al. [62] Twisted MoSe₂ bilayers with variable local stacking and interlayer coupling revealed by low-frequency Raman spectroscopy. ACS Nano. 2016;10:2736.
- Wang K, Huang B, Tian M, Ceballos F, Lin MW, Mahjouri-[63] Samani M, et al. Interlayer coupling in twisted WSe₂/WS₂ bilayer heterostructures revealed by optical spectroscopy. ACS Nano. 2016:10:6612.
- Huang J, Xiong Z, He J, Wu X, Watanabe K, Taniguchi T, et al. [64] Electrically tunable Γ-Q interlayer excitons in twisted MoSe₂ bilayers. J Mater Sci Technol. 2025;207:70-5.
- [65] Zhang Y, Baek JH, Lee CH, Jung Y, Hong SC, Nolan G, et al. Atomby-atom imaging of moiré transformations in 2D transition metal dichalcogenides. Sci Adv. 2024;10:1874.
- [66] Wu Y, Wang S, Chen C, Zhou C, Chen K, Zhou J, et al. Raman-active interlayer phonons and moiré phonons in twisted thin-layer MoTe₂. Adv Opt Mater. 2024;12:2301747.
- Kim H, Aino K, Shinokita K, Zhang W, Watanabe K, Taniguchi T, et al. Dynamics of Moiré exciton in a twisted MoSe₂/WSe₂ heterobilayer. Adv Opt Mater. 2023;11:2300146.
- [68] Wang S, Wang F, Chen C, Wu Y, Chen J, Ou H, et al. Exciton Emission in Molybdenum Telluride Homobilayers with Fine-Tuned Twist-Angles. Adv Opt Mater. 2023;11:2300424.
- leong TJ, Kim S, Choi SH. Temperature Dependence of Photoluminescence in Twisted Heterobilavers of Transition-Metal Dichalcogenides. Curr Appl Phys. 2024;60:9.
- Chen YC, Lin WH, Tseng WS, Chen CC, Rossman GR, Chen CD, et al. Direct Growth of Mm-Size Twisted Bilayer Graphene by Plasma-Enhanced Chemical Vapor Deposition. Carbon N Y. 2020;156:212.
- [71] Liu J, Zhang X, Zhang S, Zou Z, Zhang Z, Wu Z, et al. Sequential Growth and Twisted Stacking of Chemical-Vapor-Deposited Graphene. Nanoscale Adv. 2021;3:983.
- [72] Pezzini S, Mišeikis V, Piccinini G, Forti S, Pace S, Engelke R, et al. 30°-Twisted Bilayer Graphene Quasicrystals from Chemical Vapor Deposition. Nano Lett. 2020;20:3313.
- [73] Yan Z, Liu Y, Ju L, Peng Z, Lin J, Wang G, et al. Large Hexagonal Biand Trilayer Graphene Single Crystals with Varied Interlayer Rotations. Angew Chem. 2014;126:1591.
- [74] Gao Z, Zhang Q, Naylor CH, Kim Y, Abidi IH, Ping J, et al. Crystalline Bilayer Graphene with Preferential Stacking from Ni-Cu Gradient Alloy. ACS Nano. 2018;12:2275.
- Liu K, Zhang L, Cao T, Jin C, Qiu D, Zhou Q, et al. Evolution of [75] interlayer coupling in twisted molybdenum disulfide bilayers. Nat Commun. 2014;5:4966.

- Zheng H, Guo H, Chen S, Wu B, Li S, He J, et al. Strong interlayer coupling in twisted transition metal dichalcogenide Moiré superlattices. Adv Mater. 2023;35:2210909.
- [77] Bachmatiuk A, Abelin RF, Quang HT, Trzebicka B, Eckert J, Rummeli MH. Chemical vapor deposition of twisted bilayer and few-layer MoSe₂ over SiO_x substrates. Nanotechnology. 2014:25:365603.
- [78] Zheng S, Sun L, Zhou X, Liu F, Liu Z, Shen Z, et al. Coupling and interlayer exciton in twist-stacked WS₂ bilayers. Adv Opt Mater. 2015;3:1600.
- [79] Xu M, Ji H, Zhang M, Zheng L, Li W, Luo L, et al. CVD synthesis of twisted bilayer WS₂ with tunable second harmonic generation. Adv Mater. 2024;36:2313638.
- [80] Lu M, Ji H, Zhao Y, Chen Y, Tao J, Ou Y, et al. Machine learningassisted synthesis of two-dimensional materials. ACS Appl Mater Interfaces. 2022;15(1):1871-8.
- [81] Xia Y, Wu L, Wang G. Rapid evaluation method for anisotropic growth of WS2 monolayers by combining machine learning algorithms and kinetic Monte Carlo simulation data. Comput Mater Sci. 2020;184:109922.
- [82] Chen XD, Xin W, Jiang WS, Liu ZB, Chen YS, Tian JG. High-Precision Twist-Controlled Bilayer and Trilayer Graphene. Adv Mater. 2016:28:2563.
- Zhang T, Li C-H, Li W, Wang Z, Gu Z, Li J, et al. A self-healing [83] optoacoustic patch with high damage threshold and conversion efficiency for biomedical applications. Nanomicro Lett. 2024;16:122.
- [84] Kim K, Yankowitz M, Fallahazad B, Kang S, Movva HCP, Huang S, et al. Van der waals heterostructures with high accuracy rotational alignment. Nano Lett. 2016;16:1989.
- [85] Wang B, Huang M, Kim NY, Cunning BV, Huang Y, Qu D, et al. Controlled Folding of Single Crystal Graphene. Nano Lett. 2017;17:1467.
- [86] Yuan J, Liao M, Huang Z, Tian J, Chu Y, Du L, et al. Precisely controlling the twist angle of epitaxial MoS2/graphene heterostructure by AFM tip manipulation. Chin Phys B. 2022;31:087302.
- [87] Ma X, Liu Q, Xu D, Zhu Y, Kim S, Cui Y, et al. Capillary-Force-Assisted Clean-Stamp Transfer of Two-Dimensional Materials. Nano Lett. 2017;17:6961.
- [88] Tao L, Li H, Gao Y, Chen Z, Wang L, Deng Y, et al. Deterministic and etching-free transfer of large-scale 2D layered materials for constructing interlayer coupled van der waals heterostructures. Adv Mater Technol. 2018;3:1700282.
- [89] Shen PC, Lin Y, Wang H, Park JH, Leong WS, Lu AY, et al. CVD Technology for 2-D Materials. IEEE Trans Electron Devices. 2018;65:4040.
- [90] Cai Z, Liu B, Zou X, Cheng HM. Chemical vapor deposition growth and applications of two-dimensional materials and their heterostructures. Chemical reviews. 2018;118:6091-133.
- [91] Kang T, Tang TW, Pan B, Liu H, Zhang K, Luo Z. Strategies for controlled growth of transition metal dichalcogenides by chemical vapor deposition for integrated electronics. ACS materials Au. 2022:2:665-85.
- [92] Shinde SM, Dhakal KP, Chen X, Yun WS, Lee J, Kim H, et al. Stacking-controllable interlayer coupling and symmetric configuration of multilayered MoS2. NPG Asia Mater. 2018;10:1.
- [93] Wang H, Zhu D, Jiang F, Zhao P, Wang H, Zhang Z, et al. Revealing the microscopic CVD growth mechanism of MoSe₂ and the role of hydrogen gas during the growth procedure. Nanotechnology. 2018;29:314001.

- [94] Zhang Y, Lee Y, Zhang W, Song D, Lee K, Zhao Y, et al. Deterministic fabrication of twisted Van Der Waals structures. Adv Funct Mater. 2023;33:2212210.
- [95] Gan W, Han N, Yang C, Wu P, Liu Q, Zhu W, et al. A ternary alloy substrate to synthesize monolayer graphene with liquid carbon precursor. ACS Nano. 2017;11:1371.
- [96] Ma W, Zhang Q, Li L, Geng D, Hu W. Small twist, big miracle-recent progress on fabrication of twisted 2D materials. J Mater Chem C Mater. 2023;11:15793.
- [97] Gong Y, Lin J, Wang X, Shi G, Lei S, Lin Z, et al. Vertical and in-plane heterostructures from WS₂/MoS₂ monolayers. Nat Mater. 2014;13:1135.
- [98] Autere A, Jussila H, Dai Y, Wang Y, Lipsanen H, Sun Z. Nonlinear optics with 2D layered materials. Adv Mater. 2018;30:1.
- [99] Ullah K, Meng Y, Shi Y, Wang F. Harmonic Generation in Low Dimensional Materials. Adv Opt Mater. 2022;10(7):2101860.
- [100] Zhou R, Krasnok A, Hussain N, Yang S, Ullah K. Controlling the Harmonic Generation in Transition Metal Dichalcogenides and Their Heterostructures. Nanophotonics. 2022;11:3007.
- [101] Moon P, Koshino M. Optical absorption in twisted bilayer graphene. Phys Rev B Condens Matter Mater Phys. 2013;87:205404.
- [102] Ikeda TN. High-order nonlinear optical response of a twisted bilayer graphene. Phys Rev Res. 2020;2:032015.
- [103] Ha S, Park NH, Kim H, Shin J, Choi J, Park S, et al. Enhanced thirdharmonic generation by manipulating the twist angle of bilayer graphene. Light Sci Appl. 2021;10:19.
- [104] Van Der Zande AM, Kunstmann J, Chernikov A, Chenet DA, You Y, Zhang X, et al. Tailoring the Electronic Structure in Bilayer Molybdenum Disulfide via Interlayer Twist. Nano Lett. 2014:14:3869.
- [105] Paradisanos I, Raven AMS, Amand T, Robert C, Renucci P, Watanabe K, et al. Second harmonic generation control in twisted bilayers of transition metal dichalcogenides. Phys Rev B. 2022;105:115420.
- [106] Kim W, Ahn JY, Oh J, Shim JH, Ryu S. Second-Harmonic Young's Interference in Atom-Thin Heterocrystals. Nano Lett. 2020;20:8825.
- [107] Nair RR, Blake P, Grigorenko AN, Novoselov KS, Booth TJ, Stauber T, et al. Fine Structure Constant Defines Visual Transparency of Graphene. Science. 2008;320:1308.
- [108] Wang Y, Ni Z, Liu L, Liu Y, Cong C, Yu T, et al. Stacking-Dependent Optical Conductivity of Bilayer Graphene. ACS Nano. 2010;4:4074.
- [109] Agarwal H, Nowakowski K, Forrer A, Principi A, Bertini R, Batlle-Porro S, et al. Ultra-Broadband Photoconductivity in Twisted Graphene Heterostructures with Large Responsivity. Nat Photonics. 2023;17:1047.
- [110] Ni GX, Wang H, Wu JS, Fei Z, Goldflam MD, Keilmann F, et al. Plasmons in Graphene Moiré Superlattices. Nat Mater. 2015;14:1217.
- [111] Hu G, Qiu C-W, Alù A. Twistronics for Photons: Opinion. Opt Mater Express. 2021;11:1377.
- [112] Hesp NCH, Torre I, Rodan-Legrain D, Novelli P, Cao Y, Carr S, et al. Observation of Interband Collective Excitations in Twisted Bilayer Graphene. Nat Phys. 2021;17:1162.
- [113] Sunku SS, Ni GX, Jiang BY, Yoo H, Sternbach A, Mcleod AS, et al. Photonic crystals for nano-light in moiré graphene superlattices. Science. 2018;362(6419):1153–6.
- [114] Kim CJ, Sánchez-Castillo A, Ziegler Z, Ogawa Y, Noguez C, Park J. Chiral Atomically Thin Films. Nat Nanotechnol. 2016;11:520.

- [115] Chen M, Lin X, Dinh TH, Zheng Z, Shen J, Ma Q, et al. Configurable phonon polaritons in twisted α-MoO₃. Nat Mater. 2020;19:1307.
- [116] Merkl P, Mooshammer F, Brem S, Girnghuber A, Lin KQ, Weigl L, et al. Twist-tailoring coulomb correlations in van der waals homobilayers. Nat Commun. 2020;11:2167.
- [117] Stauber T, Low T, Gómez-Santos G. Plasmon-enhanced near-field chirality in twisted van der waals heterostructures. Nano Lett. 2020;20:8711.
- [118] Cong X, Liu XL, Lin ML, Tan PH. Application of Raman spectroscopy to probe fundamental properties of two-dimensional materials. npj 2D Mater Appl. 2020;4:1.
- [119] Lin KQ, Holler J, Bauer JM, Parzefall P, Scheuck M, Peng B, et al. Large-scale mapping of moiré superlattices by hyperspectral Raman imaging. Adv Mater. 2021;33:2008333.
- [120] Ribeiro HB, Sato K, Eliel GSN, De Souza EAT, Lu CC, Chiu PW, et al. Origin of van hove singularities in twisted bilayer graphene. Carbon N Y. 2015;90:138.
- [121] Papanai GS, Singh J, Sharma ND, Ansari SG, Gupta BK. Temperature dependent Raman scattering of directly grown twisted bilayer graphene film using LPCVD method. Carbon NY. 2021:177:366.
- [122] Yan W, Meng L, Meng Z, Weng Y, Kang L, Li XA. Probing angle-dependent interlayer coupling in twisted bilayer WS₂. J Phys Chem C. 2019;123:30684.
- [123] Gadelha AC, Ohlberg DAA, Rabelo C, Neto EGS, Vasconcelos TL, Campos JL, et al. Localization of lattice dynamics in low-angle twisted bilayer graphene. Nature. 2021;590:405.
- [124] Huang S, Liang L, Ling X, Puretzky AA, Geohegan DB, Sumpter BG, et al. Probing the interlayer coupling of twisted bilayer MoS₂ using photoluminescence spectroscopy. Nano Lett. 2016;16:1435.
- [125] Mallik SK, Sahoo S, Sahu MC, Jena AK, Pradhan GK, Sahoo S. Polarized moiré phonon and strain-coupled phonon renormalization in twisted bilayer MoS₂. J Phys Chem C. 2022;126:15788.
- [126] Fang T, Liu T, Jiang Z, Yang R, Servati P, Xia G. Fabrication and the interlayer coupling effect of twisted stacked black phosphorus for optical applications. ACS Appl Nano Mater. 2019;2:3138.
- [127] Saito R, Tatsumi Y, Huang S, Ling X, Dresselhaus MS. Raman spectroscopy of transition metal dichalcogenides. Journal of Physics: Condensed Matter. 2016;28:353002.
- [128] He R, Chung TF, Delaney C, Keiser C, Jauregui LA, Shand PM, et al. Observation of Low Energy Raman Modes in Twisted Bilayer Graphene. Nano Lett. 2013;13:3594.
- [129] Bin Wu J, Hu ZX, Zhang X, Han WP, Lu Y, Shi W, et al. Interface coupling in twisted multilayer graphene by resonant Raman spectroscopy of layer breathing modes. ACS Nano. 2015;9:7440.
- [130] Parzefall P, Holler J, Scheuck M, Beer A, Lin KQ, Peng B, et al. Moiré phonons in twisted MoSe₂–WSe₂ heterobilayers and their correlation with interlayer excitons. 2d Mater. 2021;8:035030.
- [131] Sun Y, Yin S, Peng R, Liang J, Cong X, Li Y, et al. Abnormal out-ofplane vibrational Raman mode in electrochemically intercalated multilayer MoS₂. Nano Lett. 2023;23:5342.
- [132] Moutinho MVO, Venezuela P, Pimenta MA. Raman Spectroscopy of Twisted Bilayer Graphene. C (Basel). 2021;7:10.
- [133] Lin M-L, Feng M, Wu J-B, Ran F-R, Chen T, Luo W-X, et al. Intralayer phonons in multilayer graphene moiré superlattices. Research. 2022;2022.
- [134] Wang S, Cui X, Jian C, Cheng H, Niu M, Yu J, et al. Stackingengineered heterostructures in transition metal dichalcogenides. Adv Mater. 2021;33:2005735. John Wiley and Sons Inc.

- [135] Campos-Delgado J, Cançado LG, Achete CA, Jorio A, Raskin JP. Raman Scattering Study of the Phonon Dispersion in Twisted Bilayer Graphene. Nano Res. 2013;6:269.
- [136] Alnasser K, Kamau S, Hurley N, Cui J, Lin Y. Resonance Modes in Moiré Photonic Patterns for Twistoptics. OSA Contin. 2021;4:1339.
- [137] He F, Zhou Y, Ye Z, Cho SH, Jeong J, Meng X, et al. Moiré patterns in 2D materials: a review. ACS nano. 2021;15:5944-58.
- [138] Gupta AK, Tang Y, Crespi VH, Eklund PC. Nondispersive Raman D band activated by well-ordered interlayer interactions in rotationally stacked bilayer graphene. Phys Rev B Condens Matter Mater Phys. 2010;82:241406.
- [139] Righi A, Costa SD, Chacham H, Fantini C, Venezuela P, Magnuson C, et al. Graphene Moiré patterns observed by umklapp double-resonance Raman scattering. Phys Rev B Condens Matter Mater Phys. 2011;84:241409.
- [140] Carozo V, Almeida CM, Ferreira EHM, Cançado LG, Achete CA, Jorio A. Raman Signature of Graphene Superlattices. Nano Lett. 2011;11:4527.
- [141] Othmen R, Arezki H, Ajlani H, Cavanna A, Boutchich M, Oueslati M, et al. Direct transfer and Raman characterization of twisted graphene bilayer. Appl Phys Lett. 2015;106:103107.
- [142] Schäpers A, Sonntag J, Valerius L, Pestka B, Strasdas J, Watanabe K, et al. Raman imaging of twist angle variations in twisted bilayer graphene at intermediate angles. 2D Mater. 2022;9:045009.
- Ramnani P, Neupane MR, Ge S, Balandin AA, Lake RK, [143] Mulchandani A. Raman Spectra of Twisted CVD Bilayer Graphene. Carbon NY. 2017;123:302.
- [144] Liu Y, Zeng C, Yu J, Zhong J, Li B, Zhang Z, et al. Moiré superlattices and related moiré excitons in twisted van der Waals heterostructures. Chem Soc Rev. 2021;50:6401-22.
- [145] Tran K, Choi J, Singh A. Moiré and beyond in transition metal dichalcogenide twisted bilayers. 2D Mater. 2021;8:022002.
- [146] Wilson NP, Yao W, Shan J, Xu X. Excitons and emergent quantum phenomena in stacked 2D semiconductors. Nat Res. 2021;599:383-92.
- [147] Shao J, Chen F, Su W, Kumar N, Zeng Y, Wu L, et al. Probing nanoscale exciton funneling at wrinkles of twisted bilayer MoS2 using tip-enhanced photoluminescence microscopy. | Phys Chem Lett. 2022:13:3304.
- [148] Peng J, Ren C, Zhang W, Chen H, Pan X, Bai H, et al. Spatially dependent electronic structures and excitons in a marginally twisted moiré superlattice of spiral WS₂. ACS Nano. 2022:16:21600.
- [149] Yuan Y, Liu P, Wu H, Chen H, Zheng W, Peng G, et al. Probing the twist-controlled interlayer coupling in artificially stacked transition metal dichalcogenide bilayers by second-harmonic generation. ACS Nano. 2023;18:17897-17907.
- [150] Zhou J, Cui J, Du S, Zhao Z, Guo J, Li S, et al. A natural indirect-todirect band gap transition in artificially fabricated MoS2 and MoSe₂ flowers. Nanoscale. 2023;15:7792.
- Huang D, Choi J, Shih CK, Li X. Excitons in semiconductor moiré superlattices. Nat Res. 2022;17:227-38.
- [152] Tartakovskii A. Excitons in 2D heterostructures. Nat Rev Phys. 2019;2(8):8-9.
- [153] Mak KF, Shan J. Semiconductor moiré materials. Nat Res. 2022;17:686-95.
- [154] Seyler KL, Rivera P, Yu H, Wilson NP, Ray EL, Mandrus DG, et al. Signatures of moiré-trapped valley excitons in MoSe₂/WSe₂ heterobilayers. Nature. 2019;567:66.

- [155] Tran K, Moody G, Wu F, Lu X, Choi J, Kim K, et al. Evidence for Moiré Excitons in van Der Waals Heterostructures. Nature. 2019;567:71.
- [156] Zhang N, Surrente A, Baranowski M, Maude DK, Gant P, Castellanos-Gomez A, et al. Moiré intralayer excitons in a MoSe₂/ MoS₂ heterostructure. Nano Lett. 2018;18:7651.
- Kremser M, Brotons-Gisbert M, Knörzer J, Gückelhorn J, Meyer M, Barbone M, et al. Discrete interactions between a few interlayer excitons trapped at a MoSe₂-WSe₂ heterointerface. NPJ 2D Mater Appl. 2020;4:8.
- [158] Förg M, Baimuratov AS, Kruchinin SY, Vovk IA, Scherzer J, Förste J, et al. Moiré excitons in MoSe2-WSe2 heterobilayers and heterotrilayers. Nat Commun. 2021;12:1656.
- [159] Shinokita K, Miyauchi Y, Watanabe K, Taniguchi T, Matsuda K. Resonant coupling of a moiré exciton to a phonon in a WSe₂/ MoSe₂ heterobilayer. Nano Lett. 2021;21:5938.
- [160] Baek H, Brotons-Gisbert M, Koong ZX, Campbell A, Rambach M, Watanabe K, et al. Highly energy-tunable quantum light from moiré-trapped excitons. Sci Adv. 2020;6:eaba8526.
- [161] Bai Y, Zhou L, Wang J, Wu W, McGilly LJ, Halbertal D, et al. Excitons in strain-induced one-dimensional moiré potentials at transition metal dichalcogenide heterojunctions. Nat Mater. 2020:19:1068.
- [162] Brotons-Gisbert M, Baek H, Campbell A, Watanabe K, Taniguchi T, Gerardot BD. Moiré-trapped interlayer trions in a charge-tunable WSe₂/MoSe₂ heterobilayer. Phys Rev X. 2021;11:031033.
- Zhang L, Zhang Z, Wu F, Wang D, Gogna R, Hou S, et al. Twist-**[163]** angle dependence of moiré excitons in WS2/MoSe2 heterobilayers. Nat Commun. 2020;11:5888.
- Liao W, Huang Y, Wang H, Zhang H. Van der waals heterostruc-[164] tures for optoelectronics: Progress and prospects. Appl Mater Today. 2019;16:435.
- [165] Lee CH, Lee GH, Van Der Zande AM, Chen W, Li Y, Han M, et al. Atomically thin P-n junctions with van der waals heterointerfaces. Nat Nanotechnol. 2014;9:676.
- [166] Xia W, Dai L, Yu P, Tong X, Song W, Zhang G, et al. Recent progress in van der Waals heterojunctions. Nanoscale. 2017;9:4324-65.
- Liu Y, Weiss NO, Duan X, Cheng HC, Huang Y, Duan X. Van der [167] Waals heterostructures and devices. Nat Rev Mater. 2016;1:1-17.
- [168] Liu L. Zhai T. Wafer-scale vertical van der Waals heterostructures. InfoMat. 2021:3:3-21.
- [169] Yin J, Wang H, Peng H, Tan Z, Liao L, Lin L, et al. Selectively enhanced photocurrent generation in twisted bilayer graphene with van Hove singularity. Nat Commun. 2016;7:10699.
- Tan Z, Yin J, Chen C, Wang H, Lin L, Sun L, et al. Building Large-Domain Twisted Bilayer Graphene with van Hove Singularity. ACS Nano. 2016;10:6725.
- [171] Xin W, Chen XD, Liu ZB, Jiang WS, Gao XG, Jiang XQ, et al. Photovoltage Enhancement in Twisted-Bilayer Graphene Using Surface Plasmon Resonance. Adv Opt Mater. 2016;4:1703.
- Turunen M, Brotons-Gisbert M, Dai Y, Wang Y, Scerri E, Bonato C, [172] et al. Quantum photonics with layered 2D materials. Nat Rev Phys. 2022;4:219-36.
- Seifert P, Lu X, Stepanov P, Durán Retamal JR, Moore JN, Fong KC, [173] et al. Magic-angle bilayer graphene nanocalorimeters: Toward broadband, energy-resolving single photon detection. Nano Lett.
- [174] Lu X, Stepanov P, Yang W, Xie M, Aamir MA, Das I, et al. Superconductors, orbital magnets and correlated states in magicangle bilayer graphene. Nature. 2019;574:653.

- [175] Sunku SS, Halbertal D, Stauber T, Chen S, McLeod AS, Rikhter A, et al. Hyperbolic enhancement of photocurrent patterns in minimally twisted bilayer graphene. Nat Commun. 2021;12:1641.
- [176] Hesp NCH, Torre I, Barcons-Ruiz D, Herzig Sheinfux H, Watanabe K, Taniguchi T, et al. Observation of interband collective excitations in twisted bilayer graphene. Nat Commun. 2021:12:1162–8.
- [177] Paik EY, Zhang L, Burg GW, Gogna R, Tutuc E, Deng H. Interlayer exciton laser of extended spatial coherence in atomically thin heterostructures. Nature. 2019;576:80.
- [178] Jiang Y, Chen S, Zheng W, Zheng B, Pan A. Interlayer exciton formation, relaxation, and transport in TMD van der Waals heterostructures. Light Sci Appl. 2021;10:72.
- [179] Pei D, Zhou Z, He Z, An L, Gao H, Xiao H, et al. Twist-induced modification in the electronic structure of bilayer WSe₂. Nano Lett. 2023;23:7008.
- [180] Molino L, Aggarwal L, Maity I, Plumadore R, Lischner J, Luican-Mayer A. Influence of atomic relaxations on the moiré flat band wave functions in antiparallel twisted bilayer WS₂. Nano Lett. 2023;23:11778.
- [181] Sun X, Suriyage M, Khan AR, Gao M, Zhao J, Liu B, et al. Twisted van der waals quantum materials: Fundamentals, tunability, and applications. Chem Rev. 2024;124:1992.
- [182] Lim SY, Kim HG, Choi YW, Taniguchi T, Watanabe K, Choi HJ, et al. Modulation of phonons and excitons due to moiré potentials in twisted bilayer of WSe₂/MoSe₂. ACS Nano. 2023;17:13938.
- [183] Jin C, Ma EY, Karni O, Regan EC, Wang F, Heinz TF. Ultrafast dynamics in van der Waals heterostructures. Nat Nanotechnol. 2018;13:994–1003.

- [184] Yu H, Peng Y, Yang Y, Li ZY. Plasmon-enhanced light–matter interactions and applications. npj Comput Mater. 2019;5:45.
- [185] Meng Y, Feng J, Han S, Xu Z, Mao W, Zhang T, et al. Photonic van der Waals integration from 2D materials to 3D nanomembranes. Nat Rese. 2023;8(8):498–517.
- [186] Joannopoulos JD, Villeneuve PR, Fan S. Photonic crystals: putting a new twist on light. Nature. 1997;13;386(6621):143–9.
- [187] Saumya K, Naskar S, Mukhopadhyay T. 'Magic' of twisted multilayered graphene and 2D nano-heterostructures. Nano Futures. 2023;7:032005.
- [188] Shi B, Qi P, Jiang M, Dai Y, Lin F, Zhang H, et al. Exotic physical properties of 2D materials modulated by moiré superlattices. Mater Adv. 2021;2:5542–59.
- [189] Reidy K, Varnavides G, Thomsen JD, Kumar A, Pham T, Blackburn AM, et al. Direct imaging and electronic structure modulation of moiré superlattices at the 2D/3D interface. Nat Commun. 2021;12:1290.
- [190] Claassen M, Xian L, Kennes DM, Rubio A. Ultra-strong spin–orbit coupling and topological moiré engineering in twisted ZrS₂ bilayers. Nat Commun. 2022;13:4915.
- [191] Lu X, Lian B, Chaudhary G, Piot BA, Romagnoli G, Watanabe K, et al. Multiple flat bands and topological Hofstadter butterfly in twisted bilayer graphene close to the second magic angle. Proc Natl Acad Sci. 2021;118:2021.
- [192] Yang Y, Ge Y, Li R, Lin X, Jia D, Guan Y, et al. Demonstration of negative refraction induced by synthetic gauge fields. Sci Adv. 2021;7:eabj2062.
- [193] Hu J, Tan J, Al Ezzi MM, Chattopadhyay U, Gou J, Zheng Y, et al. Controlled alignment of supermoiré lattice in double-aligned graphene heterostructures. Nat Commun. 2023;14(1):4142.